ELABORATION OF THE MATRIX GLYCOPROTEIN OF ENAMEL BY THE SECRETORY AMELOBLASTS OF THE RAT INCISOR AS REVEALED BY RADIOAUTOGRAPHY AFTER GALACTOSE-3H INJECTION

ALFRED WEINSTOCK and C. P. LEBLOND

From the Department of Anatomy, McGill University, Montreal, Canada. Dr. Weinstock's present address is the Departments of Periodontology and Anatomy, Schools of Dentistry and Medicine, The Center for the Health Sciences, University of California, Los Angeles, California 90024

ABSTRACT

The elaboration of enamel matrix glycoprotein was investigated in secretory ameloblasts of incisor teeth in 30–40-g rats. To this end, the distribution of glycoprotein was examined histochemically by the use of phosphotungstic acid at low pH, while the formation of glycoprotein was traced radioautographically in animals sacrificed 2.5–30 min after galactose-3H injection. Histochemically, the presence of glycoprotein is observed in ameloblasts as well as in the enamel matrix; in ameloblasts glycoprotein occurs within the Golgi apparatus in amounts increasing from the outer to the inner face of the stacks of saccules, and is concentrated in condensing vacuoles and secretory granules; in the enamel matrix, glycoprotein is observed within linear subunits. Radioautographs at 2.5 min after injection demonstrate the uptake of galactose-3H label by Golgi saccules, indicating that galactose-3H is incorporated into glycoprotein within this organelle. After 5–10 min, the label collects in the condensing vacuoles and secretory granules of the Golgi region. By 20–30 min, the label appears in the secretory granules of the apical (Tomes') processes, as well as in the enamel matrix (next to the distal end of the apical processes, and at the tips of matrix prongs). In conclusion, galactose contributes to the formation of glycoprotein within the Golgi apparatus. The innermost saccules then distribute the completed glycoprotein to condensing vacuoles, which later evolve into secretory granules. These granules rapidly migrate to the apical processes, where they discharge their glycoprotein content to the developing enamel.

INTRODUCTION

The enamel matrix of the rat incisor is elaborated by the tall "secretory" ameloblasts. Soon after its deposition next to the apical (Tomes') processes, the matrix becomes calcified. While much is known of the structure of these ameloblasts, particularly in the incisor teeth of rat (1–9) and mouse (10, 11), their mode of secretion and their control of calcification are little understood. The present investigation approached the problem of matrix secretion by taking advantage of the presence of glycoprotein within the enamel matrix (12–17). In a first step, the histochemical localization of this glycoprotein was attempted, both within ameloblasts as well as in enamel matrix, by

the use of phosphotungstic acid (18–20) at low pH according to Rambourg (21, 22).

The next step was to examine the formation of the carbohydrate moiety of the matrix glycoprotein. The presence of galactose in this glycoprotein (14, 16, 17) led us to inject tritium-labeled galactose into young rats and trace it within the ameloblasts and enamel of incisor teeth by means of radioautography.[1]

In the course of this work, cytological observations were made on the Golgi apparatus and the apical (Tomes') process of ameloblasts. Correlation of these observations with histochemical and radioautographic results provided some insight into the mechanism by which ameloblasts elaborate and deposit the matrix of developing enamel.

MATERIALS AND METHODS

Administration of Galactose-^{3}H and Fixation of Tissues

Male Sherman rats weighing 30–40 g each were anesthetized with ether. 5 mCi of D-galactose-1-^{3}H (SA 1.17 Ci/mmole, Amersham-Searle Corp., Des Plaines, Ill.) were injected into the external jugular vein of each. The labeled galactose provided in distilled water was concentrated in a Flash Evaporator (Buchler Instruments, Inc., Fort Lee, N. J.) immediately before use. The final volume was 0.15–0.2 ml/animal. After 2.5, 5, 10, or 30 min, the animals were sacrificed by intracardiac perfusion with glutaraldehyde. In the case of those animals which were sacrificed 2.5 min after injection, the trachea was first intubated with a polyethylene catheter (Venocath-16, No. 4816, Abbott Laboratories, North Chicago, Ill.); the animals were then kept under ether until perfusion was started. Those animals which were sacrificed 5, 10, or 30 min after injection were reanesthetized just before perfusion and intubated at that time. In both cases, the tracheotomy tube was connected to a tank which provided a 95% O_2 + 5% CO_2 mixture, while a shunt allowed the operator to direct the gas flow through a vessel containing ether whenever the depth of anesthesia had to be increased.

Perfusion was done at room temperature with a solution of 2.5% glutaraldehyde (TAAB Laboratories, Emmer Green, Reading, England) in 0.05 M phosphate buffer (Sörensen) at pH 7.2 with 0.1% sucrose and 1% galactose added (final osmolality, about 470 mosmols). This mixture was injected through the left ventricle of the heart by means of a

[1] Preliminary results of this work were presented earlier (79).

polyethylene catheter (Venocath-16) attached to a Ministaltic Pump (Manostat Corp., New York) preset at a dial reading of 0.3. After 5 min, the pump was turned off and the fixative was allowed to continue flowing by gravity at the rate of about 60 drops/min for an additional 15 min.

The maxillary incisor teeth were dissected from the maxillae and immersed in fresh fixative for an additional 2 hr at 4°C. They were then demineralized in disodium ethylenediamine tetraacetate (EDTA) by

TABLE I

Relative Volumes, as Estimated by the Percentage of "Hits" (reference 30) in the Supranuclear Region of Secretory Ameloblasts

100–225 hits in each of 100 micrographs from four animals are represented.

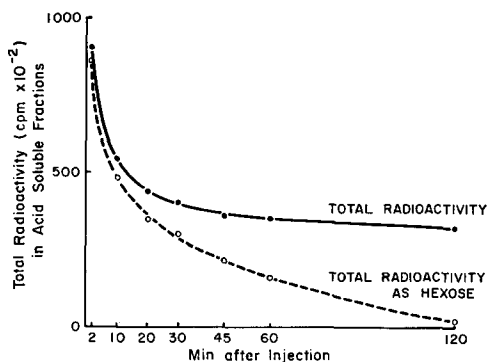|	Relative volume
	%
Golgi apparatus	43
rER	48
Condensing vacuoles	1.2
Secretory granules	1.1
Dense bodies	1.7
Plasma membrane	5.1

FIGURE 1 Variation in the radioactivity of blood plasma with time after intravenous injection of galactose-^{3}H into 300–400-g rats. Values for intervals 2–60 min after injection represent averages of samples from two animals, whereas the 120 min values come from only one animal. The "total radioactivity" is the amount present in the supernatant fraction after precipitation of plasma proteins with trichloroacetic and phosphotungstic acid. The "total radioactivity as hexose" refers to the sum of the radioactivities recovered as galactose, glucose, and mannose, after correction for a 5% loss in recovery from paper chromatograms. The radioactivity present as hexose decreases rapidly with time to become negligible by 120 min.
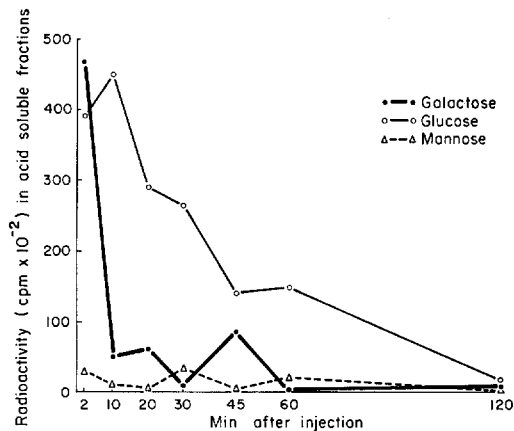
FIGURE 2 Radioactivity present as galactose, glucose, and mannose in blood plasma at various times after injection of galactose-^{3}H into 300–400-g rats. Within 2 min after injection of galactose-^{3}H, about half of the plasma hexose radioactivity is present in glucose; within 10 min, most of the radioactivity is in glucose. Only a small amount passes into mannose. It appears that injected galactose rapidly disappears from the blood.

the method of Warshawsky and Moore (23) for 2 wk at 4°C. (It is believed that the EDTA treatment of fixed tissues did not extract labeled material; it was noteworthy that the radioautographic patterns of the soft tissues surrounding the teeth were the same whether or not they had been subjected to EDTA treatment.)
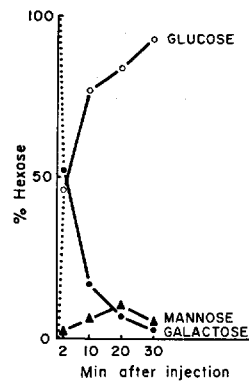
FIGURE 3 Percentage of the hexose radioactivity present as galactose, glucose, or mannose at various time intervals after injection of galactose-^{3}H into 30–40-g rats. Again, radioactivity passes from galactose to glucose, while galactose rapidly disappears from the blood.

Demineralization was followed by an overnight rinse in 0.15 M Sörensen phosphate buffer at pH 7.2. The incisor teeth were then sliced transversely into 1-mm thick sections and immersed into 1% osmium tetroxide in 0.1 M phosphate buffer at 4°C for 1.5 hr. The specimens were then dehydrated in a graded series of acetone solutions at room temperature, and flat-embedded in Epon in inverted BEEM capsules (Better Equipment for Electron Microscopy, Bronx, N.Y.).

FIGURE 4 A rat maxillary incisor tooth as seen in a semithin transverse section through the region of enamel matrix secretion (within the proximal 1/3 of the tooth). Toluidine blue stain. The enamel organ is located on the labial surface of the incisor (lowermost part of figure). From the base up, the lettering points to the layer of secretory ameloblasts (A), the enamel matrix (E) intensely stained by toluidine blue, the dentin (D) separated from the layer of odontoblasts (O) by the lightly staining predentin, and finally the pulp (P). × 60.

FIGURE 5 Secretory ameloblasts as they appear in a semithin transverse section through the region of enamel matrix secretion in a rat maxillary incisor. The ameloblasts from the base up show a faintly visible basal web (B), the groups of mitochondria intensely stained with toluidine blue (M), the elongated nucleus, the supranuclear cytoplasm with the Golgi apparatus appearing as a double stranded structure (G), the terminal web (W), and the apical or Tomes' process (Ap) which is partially embedded in the enamel matrix. The toluidine blue-stained content of the apical process represents secretory granules (cf. Figs. 5 and 6). Since the apical processes of ameloblasts in a given row interdigitate with those in other rows, the cut-off portions of several rows of processes are visible. SI, stratum intermedium. × 1000.

FIGURE 6 A diagrammatic representation of the structure of a secretory ameloblast from the region of enamel matrix secretion in a rat maxillary incisor. Mitochondria are usually grouped between basal web and nucleus. The supranuclear region contains an elongated tubular-shaped Golgi apparatus which is surrounded on all sides by rER. Within the central core of cytoplasm demarcated by the Golgi saccules are condensing vacuoles and a few secretory granules. The apical process extends apically from the terminal web and its distal portion is embedded in the enamel matrix. Secretory granules abound within its central core. The "growth regions" represent the most recently deposited matrix, as described in the text.
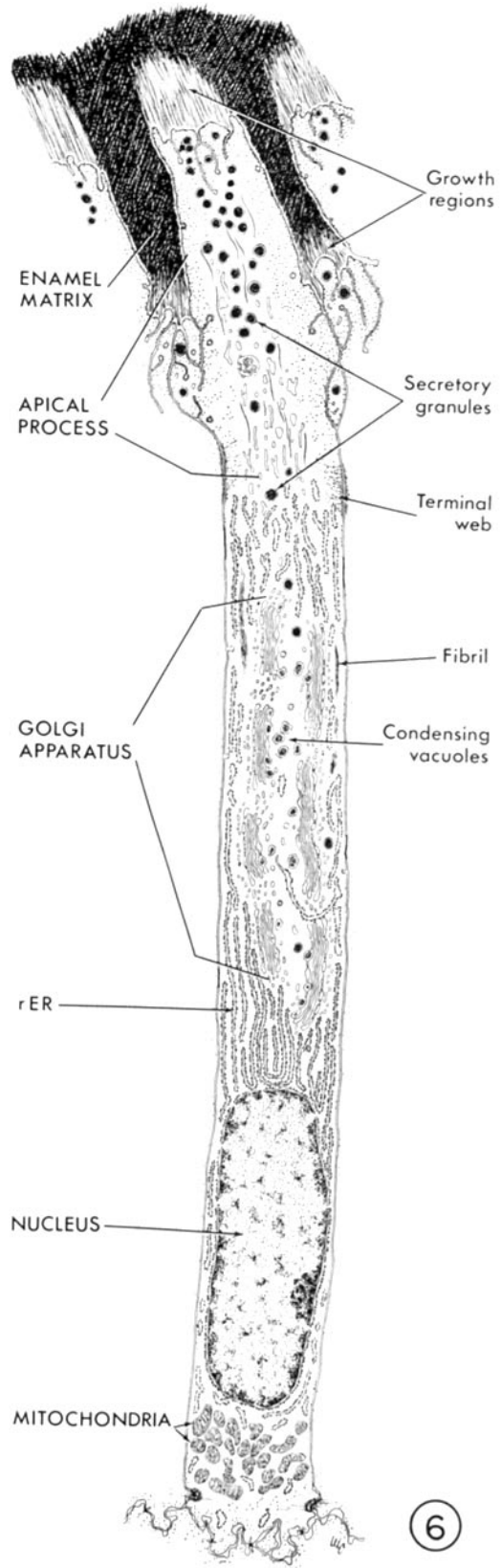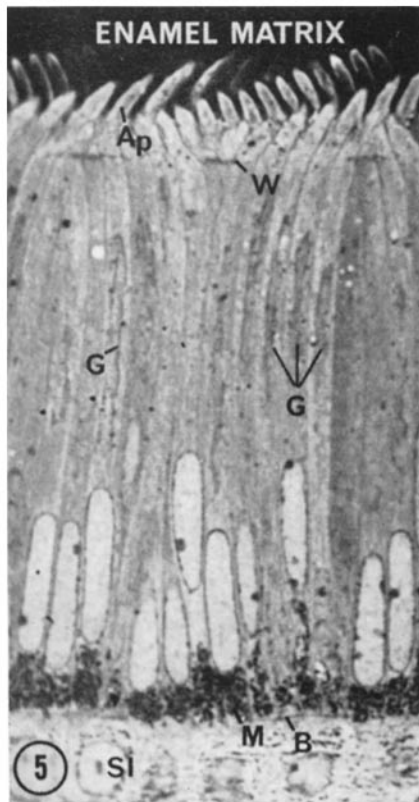
For electron microscopy, ultrathin sections (pale gold to silver interference colors) were treated with lead citrate (24) for 8 min and subsequently examined in a Siemens Elmiskop I or Hitachi HS-7S electron microscope.

Mandibles including the lower incisor teeth were postfixed in Bouin's fluid for 24 hr after glutaraldehyde fixation and demineralized as above. They were subsequently sliced transversly with razor blades. The slices were then embedded in a celloidin-paraffin medium for light microscopy.

Radioautography

With a wire loop, ultrathin sections were placed on glass microscope slides coated with celloidin (0.8% in isoamylacetate). With the aid of the semiautomatic device of Kopriwa (25), the slides were dipped into Ilford L4 emulsion (Ilford Ltd., Ilford, Essex, England) diluted 1:3 with distilled water. After exposure times ranging from 3 to 9 months at 4°C, the radioautographs were developed in D19b for 1–2 min at 20°C (26), or Elon-ascorbic acid (Eastman Kodak Corp., Rochester, N.Y.) for 6–8 min at 24°C after gold latensification (27), and subsequently fixed for 2 min in 24% sodium thiosulfate. As a rule, the radioautographs were stained only with lead citrate for 20–30 min (24) before examination in the electron microscope.

For light microscope radioautography, 4-μ thick paraffin or 1-μ thick Epon sections were mounted on glass microscope slides and dipped in Kodak NTB2 emulsion (28). After exposure times ranging from 2 wk to 4 months at 4°C, the radioautographs were developed in D170 for 6 min at 18°C (29), followed by fixation for 3 min in 24% sodium thiosulfate. Paraffin sections were then stained with hematoxylin and eosin, and Epon sections with 1% toluidine blue in a saturated borax solution.

Quantitative Radioautography

Three areas of the secretory ameloblast were considered: the infranuclear region, the supranuclear (Golgi) region, and the apical (Tomes') process with the associated matrix. Since the infranuclear region was essentially unlabeled at early intervals after injection and showed only a light scattered reaction at 30 min, quantitation of silver grains was not carried out in micrographs of this area. The supranuclear region was reactive at all time intervals under study and its reactions were quantified. The apical process was unreactive at 2.5, 5, and 10 min, but was intensely reactive at 30 min; at this last time interval the reactions in the supranuclear and apical process regions were given equal weighting to obtain combined values.

Quantitation was done by counting the silver

FIGURE 7   This and all other electron micrographs are of longitudinally cut secretory ameloblasts and, unless otherwise indicated, are stained with lead citrate. Supranuclear Golgi region. Three cells are separated by their respective cell membranes (CM). The Golgi apparatus of the central cell is composed of a double array of stacks of saccules running parallel to the long axis of the cell. It is surrounded on either side by microtubules (MT) and profiles of rER. Between the Golgi apparatus and rER are numerous small vesicles referred to as intermediate vesicles (I) (see also I in the cell at left). The central core of cytoplasm demarcated by the Golgi stacks may contain condensing vacuoles identified by their relatively thick, uneven halo and loosely applied limiting membrane (CV), secretory granules with a tightly applied limiting membrane (G), and bristle-coated vesicles (V), some of which are also present at lower right adjacent to or continuous with the plasma membrane. A cytoplasmic fibril composed of densely packed filaments is shown at F (upper center). Arrows point to scattered glycogen granules. × 27,000.

FIGURE 8   Golgi region. The two arrays of Golgi saccules occupy the central portion of the figure, with profiles of rER on both sides. Intermediate vesicles (I) predominate in the space between Golgi apparatus and rER. At upper right, a cisterna shows a ribosome-free region displaying buds coated with a fine-textured fuzz (arrows). Some of the intermediate vesicles in the immediate vicinity and others scattered between rER and Golgi apparatus at left demonstrate a similar external fuzz. Finally, similar buds are attached to Golgi saccules (arrows at upper and lower left). The Golgi saccules at left (S_1, S_2) are obliquely sectioned, and one displays distinct fenestrations (lower left, S_2). Each fenestration appears to contain a central density. In the axial core of cytoplasm, free condensing vacuoles (CV) in various developmental stages consist of a droplet of finely granular or sometimes homogeneous material which is surrounded by a loosely applied limiting membrane. An electron-lucent halo of variable thickness usually separates the membrane from the internal content. It is not uncommon to observe localized areas of bristle-like material on the outer surface of the membrane (arrowhead). This coating material resembles the surface coating observed on bristle-coated vesicles (V). G, secretory granule. × 45,000.
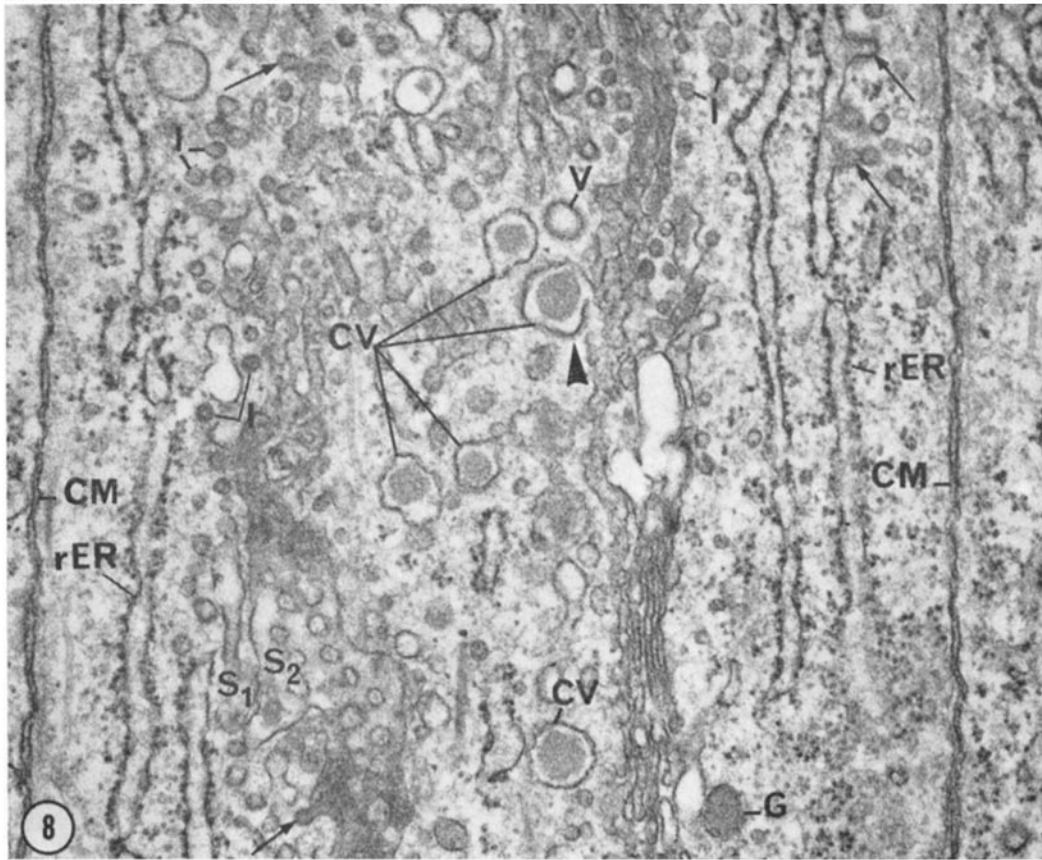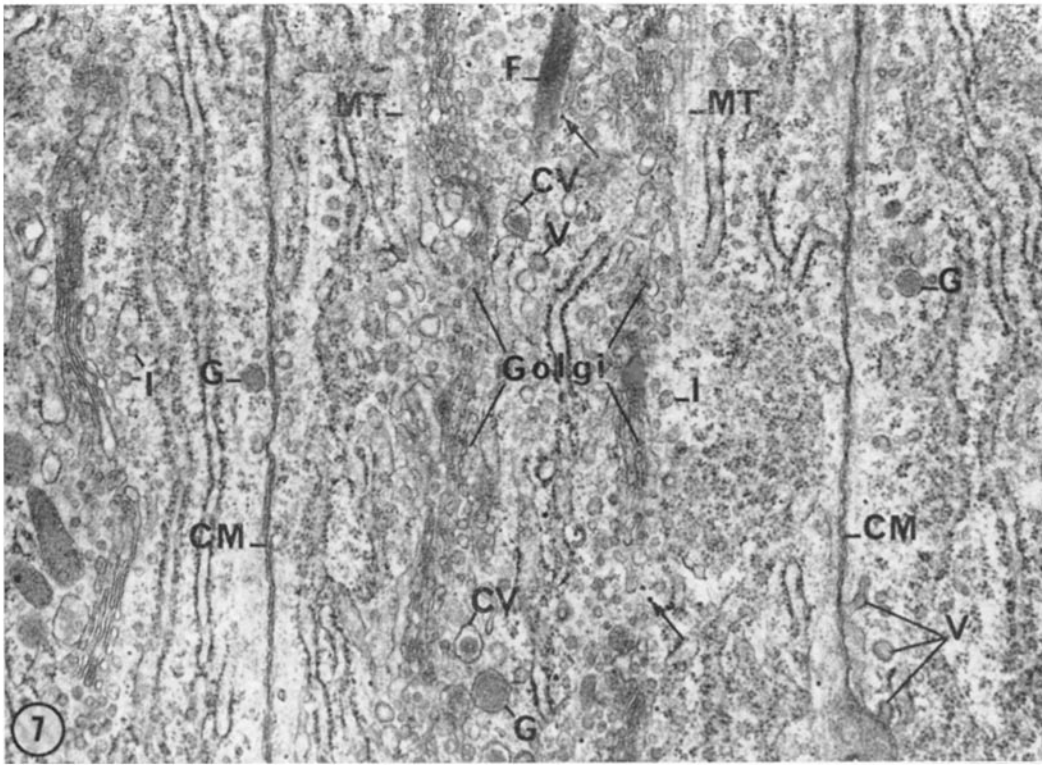
grains directly overlying the following cell structures in micrographs of specimens magnified to 30,000 diameters: (a) Golgi apparatus and associated vesicles, (b) secretory granules (including condensing vacuoles), (c) rough endoplasmic reticulum (rER), and (d) other structures. When a grain overlapped the Golgi apparatus and rER, it was assigned to the predominant structure under the grain, but when a grain overlapped a secretory granule or condensing vacuole and another structure, it was assigned to the granule or condensing vacuole.

In order to assess the significance of the reaction over the various components of the supranuclear (Golgi) region of ameloblasts, the relative volumes of these components were measured by the "point-hit" method of Chalkley (30, 31), as recorded in Table I.

Radioautography after Glucose-³H Injection

5 mCi of glucose-³H (SA 1.2 Ci/mmole; Amersham-Searle Corp., Des Plaines, Ill.) were injected into each of three animals under conditions identical to those used for galactose-³H. The animals were sacrificed 2.5, 5, and 20 min later, and radioautographs were prepared.

Variation in Blood Plasma Radioactivity with Time after Galactose-³H Injection

Blood plasma clearance curves were determined by injecting 100 μCi (0.1 ml) of D-galactose-1-³H

(SA 1.17 Ci/mmole, Amersham-Searle Corp.) into the jugular vein of each of two rats weighing 300–400 g each under Nembutal anesthesia (Abbott Laboratories, 5 mg/100 g body weight). Animals of this size were used in order to obtain successive blood samples from a given animal. The samples (0.4–0.5 ml) were withdrawn from the external jugular vein at time intervals ranging from 2 to 120 min after injection. Proteins and glycoproteins were precipitated from the plasma at 4°C overnight by the use of a solution of 10% trichloroacetic acid + 0.85% phosphotungstic acid. After thrice rinsing the precipitates, 100-μl samples of the supernate (acid soluble) fractions were added to vials containing 15 ml of Bray's solution (34). Radioactivity was monitored in a Packard Tri-Carb, Model 3003, liquid scintillation spectrometer (Fig. 1).

Galactose, glucose, and mannose were separated from the supernate fraction of each blood plasma sample by paper chromatography with the use of 23 cm × 57 cm sheets of No. 1 Whatman Chromatography Paper. A mixture of standard hexoses dissolved in the same acids was spotted on both sides of the chromatograms, each spot containing 100-150 μg of each hexose, and the supernate fractions were then streaked between the standard spots. After drying under an air stream at room temperature, the chromatograms were developed in a descending system with the use of ethyl acetate:water:pyridine in a proportion of 2:2:1 (v:v:v) for a duration of 24–30 hr at room temperature (35). After air drying, reducing sugars were detected by spraying the

FIGURE 9   Golgi region, showing a single array of saccules on the left side of the cell only. In the center, a string of five "droplets" of electron-opaque material within an innermost saccule represents saccule-bound condensing vacuoles. The saccular membrane applies itself to the contour of each droplet, thus producing a beadlike arrangement with membrane constrictions occurring between droplets (arrows). By comparison with the free condensing vacuoles depicted in Fig. 8, it appears that the five droplets will free themselves from the saccule. The array of Golgi stacks on the right side of the cell is interrupted, but a portion is visible at the top (right of center). In the axial core of cytoplasm (top center), a cisterna of rough ER (rER) is seen next to intermediate vesicles. Finally, large bristle-coated vesicles (V), a tangential section through a condensing vacuole (CV*), and a dense body (DB) may also be seen. The tangentially sectioned surfaces of rER cisternae to the left of the Golgi apparatus display coil-shaped polyribosomal configurations (arrowheads) which may exhibit as many as 17 ribosomes along their lengths. × 36,000.

FIGURE 10   Stack of Golgi saccules. From the left, one may see two adjacent cell membranes and a few cisternae of rER. (Some rER cisternae are applied to the plasma membranes, in which instance ribosomes are lacking on the applied surface.) A few intermediate vesicles are seen at lower left (I). Two buds with a fine fuzzy coating (arrows) are seen on the discontinuous outermost Golgi saccule (S₁). The second saccule (S₂) is fenestrated and thick but lacks discernible content while some content may be distinguished in saccules S₃-S₅. CV, condensing vacuole. × 60,000.

FIGURE 11   Golgi region. The upper two condensing vacuoles share a common limiting membrane, presumably due to their having not yet separated from their mother saccule and being, therefore, saccule-bound. The lowest condensing vacuole appears to be free. The limiting membrane belonging to one of the saccule-bound condensing vacuoles shows coated buds (arrows). The material contained within both types of condensing vacuole has a density and texture somewhat similar to that seen within the Golgi saccules (S) at upper right. V, bristle-coated vesicles. × 60,000.

33
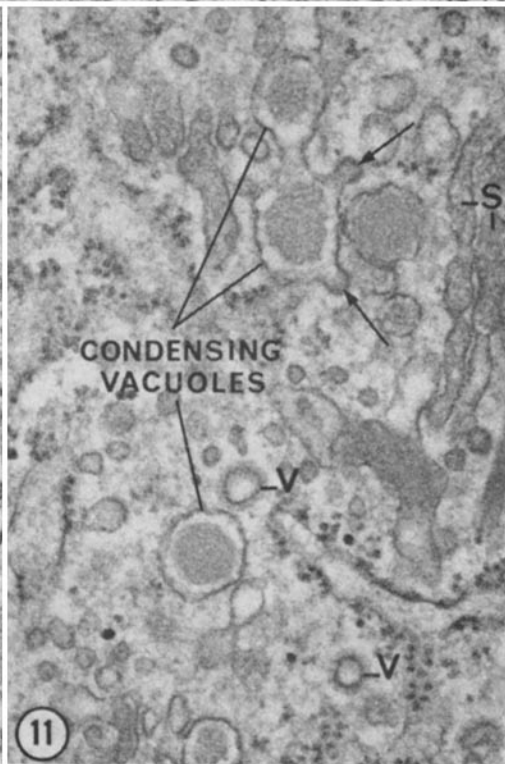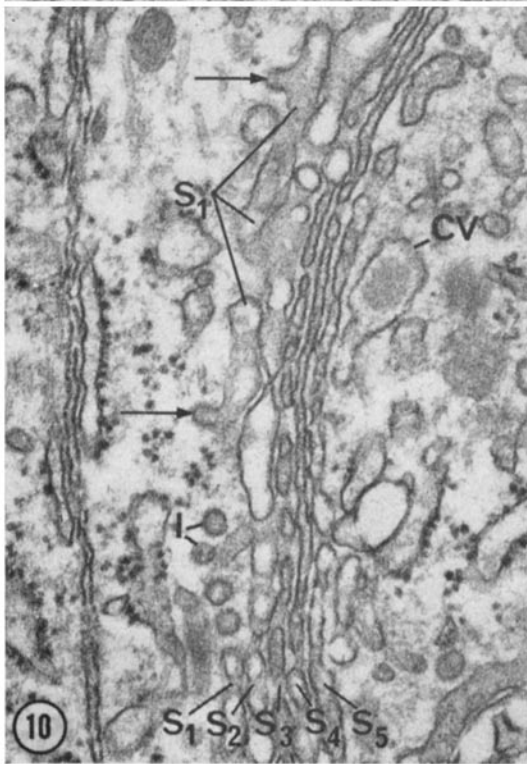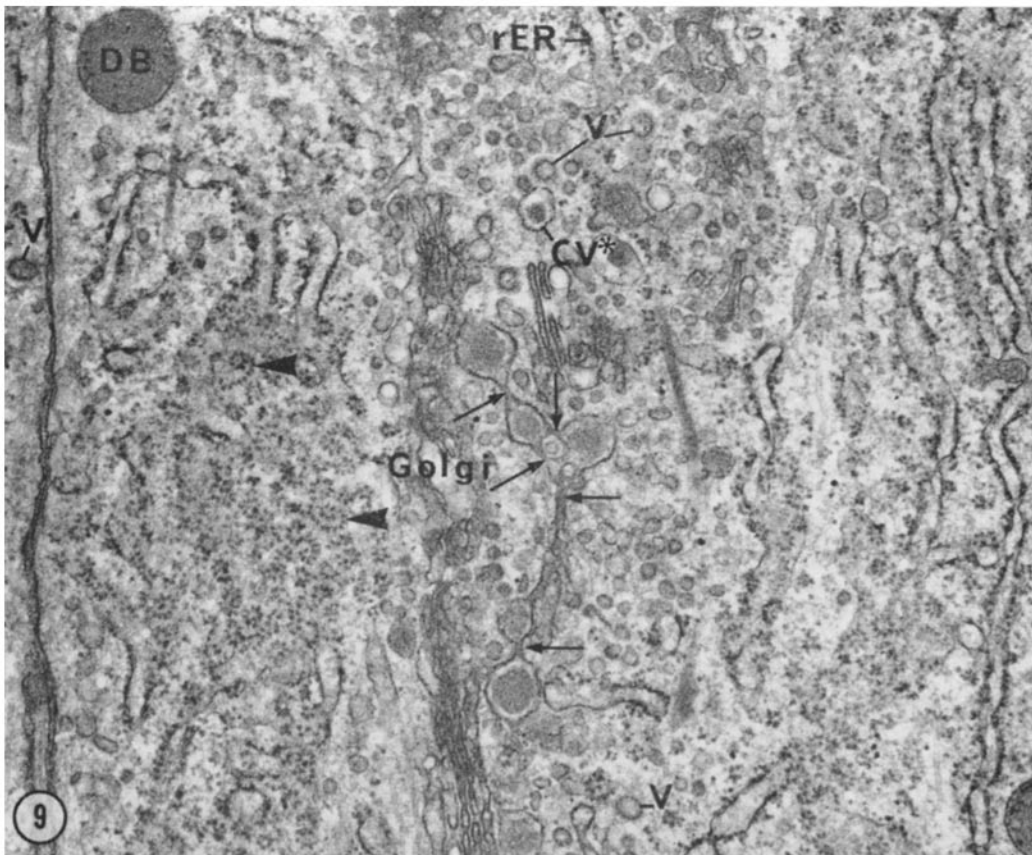
chromatograms with a fresh solution of 1% *p*-anisidine hydrochloride (Eastman Organic Chemicals, Div. of Eastman Kodak Co., Rochester, N. Y.) in *n*-butanol (36), followed by heating in an oven for 7–10 min at 105–110°C. Aldohexoses appeared as brown spots. Strips of paper between spots were cut out, placed in separate 50-ml Erlenmeyer flasks containing 15 ml of distilled water, and shaken in a water bath for 2 hr at 37°C. This elution was twice repeated for 1 hr each, with heating omitted in the last elution. The pooled extracts were evaporated to dryness in a Flash Evaporator at 35°C, the residues were redissolved in 2–5 ml of distilled water, and a sample of each was monitored on a liquid scintillation spectrometer by the use of Bray's solution. Recovery of radioactivity was 90–95%. The results are presented in Fig. 2.

These experiments were repeated in rats of the size used for radioautography (30–40 g each). Each of eight animals received 50 μCi (0.05 ml) of galactose-^{3}H in the external jugular vein. At 2, 10, 20, and 30 min after injection, 0.5 ml of blood was withdrawn from the inferior vena cava of each of two rats at each postinjection interval, and the blood samples were processed as described above. The results are presented in Fig. 3.

Histochemical Detection
of Glycoprotein

Demineralized, glutaraldehyde-fixed incisor teeth were embedded in glycol methacrylate (32) and stained with phosphotungstic acid kept at low pH by addition of chromic or hydrochloric acid as suggested by Rambourg (21, 22). Ultrathin sections were prepared and transferred by means of plastic loops to a small Petri dish containing a freshly prepared, filtered solution of 1% phosphotungstic acid in 1 N HCl. After 1 hr the sections were floated on distilled water for a few seconds and rapidly transferred to copper grids.

Glycogen Extraction with Amylase

To remove glycogen, 1-mm thick sections of demineralized, paraformaldehyde-fixed (4% paraformaldehyde in 0.1 M phosphate buffer) incisor teeth were incubated at 37°C for 1 hr in a 0.01 M phosphate-buffered 1% solution of α-amylase (Worthington Biochemical Corp., Freehold, N.J.; hog pancreas, twice crystallized, activity 666 U/mg) with the use of a shaker-type water bath (33). After a brief buffer rinse the sections were fixed in osmium tetroxide and embedded in Epon as described above. Since ameloblasts contain only small quantities of glycogen, the efficiency of the method was tested on 1-mm³ blocks of liver incubated in the same flask. These blocks lost their glycogen following the digestion procedure. Control ameloblasts and liver sections were incubated in the buffer solution without enzyme added. This method was applied to an animal sacrificed 10 min after injection of galactose-[3]H.

RESULTS

STRUCTURE OF THE SECRETORY AMELOBLAST WITH
SPECIAL REFERENCE TO THE GOLGI
APPARATUS AND THE
APICAL PROCESS

The secretory ameloblasts of the rat maxillary lincisor are arranged in a single layer on the labia

FIGURE 12 Apical (Tomes') processes and associated enamel matrix. The *proximal* portion of each process (lower 1/3 of the micrograph) contains scattered secretory granules (*G*) as well as smooth membranous elements (*S*) admixed with fragments of rER, microtubules (*MT*), bristle-coated vesicles (*V*) and a few glycogen granules (arrows). The *distal* portion of each apical process (upper ⅔ of micrograph) is embedded within enamel matrix. Each process is limited by a plasma membrane which is closely applied to the matrix. At the distal end, the plasma membrane is thrown into folds which invaginate inwards (see arrows at tip of each process). Invaginations are infrequent along the lateral aspects of a process. Secretory granules abound within the central core of the processes, in association with microtubules and smooth membranous elements. The core of cytoplasm containing the secretory granules is usually ensheathed by a feltwork of fine filaments (*f*) which extends to the plasma membrane. The junction between the proximal and distal regions is indicated by the tips of the enamel prongs. There the cell membrane is thrown into elaborate infoldings (arrows, lower left). Although the enamel matrix appears relatively homogeneous at this magnification, it shows an arrangement of parallel lines in two regions: (*a*) the matrix abutting the distal end of each process (**, upper left), and (*b*) at the proximal ends of the prongs of matrix (*) projecting between the processes. These are the two regions where the nearby plasma membrane shows numerous infoldings (arrows). × 21,000.

Electron micrographs of secretory ameloblasts embedded in glycol methacrylate and "stained" with phosphotungstic acid at low pH for the detection of glycoprotein. × 45,000.

ENAMEL MATRIX
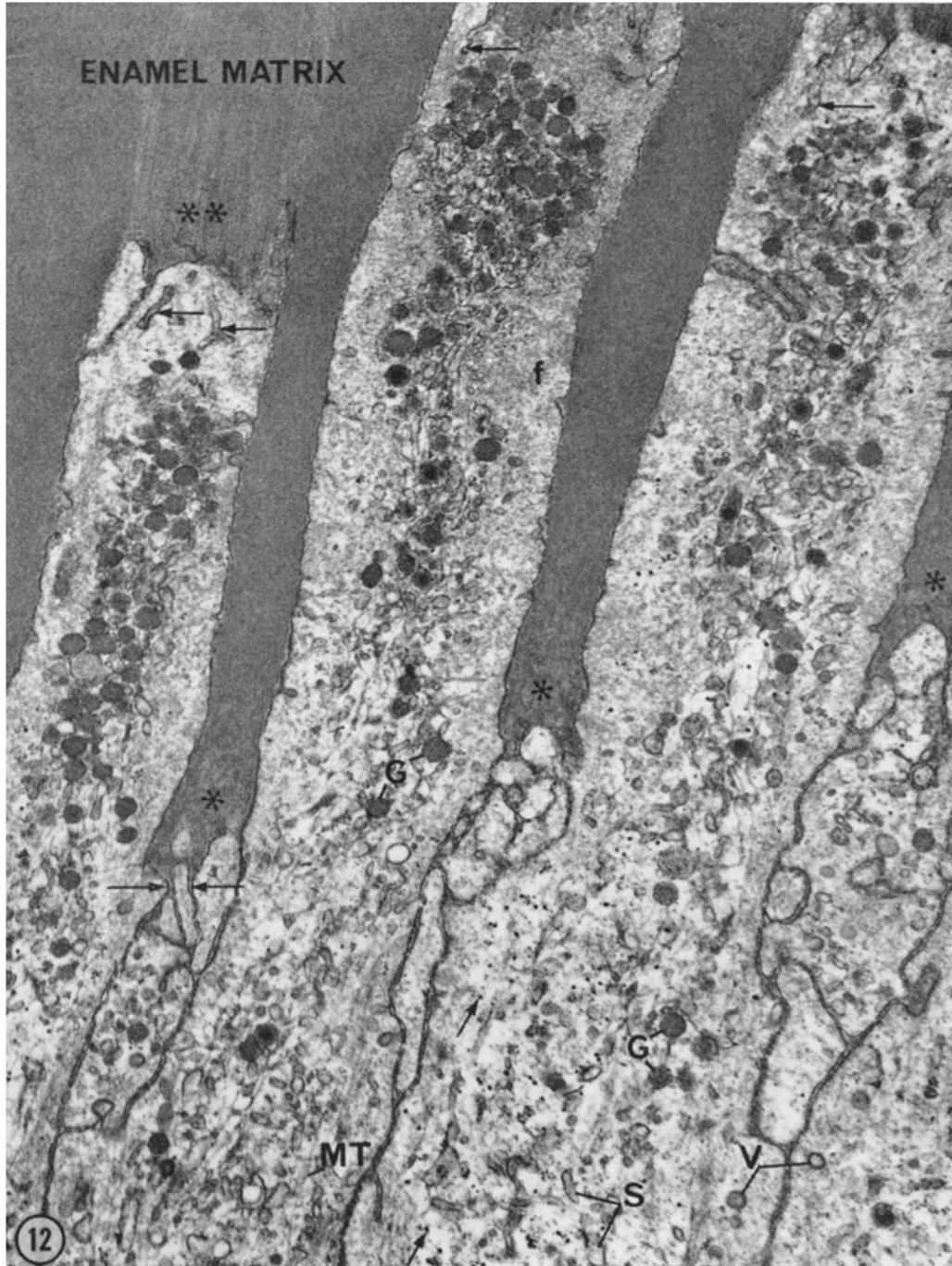
surface of the tooth[2] (Fig. 4). They are tall columnar cells (about 50 μ in height) in which the organelles are precisely segregated (Fig. 5). Mitochondria are grouped below the nucleus at the base of the cell.

Above the nucleus, a tubular-shaped Golgi apparatus (7) is visible as a double-stranded structure running longitudinally along the cell axis (Figs. 5, 6). Between the Golgi apparatus and the plasma membrane, there are narrow cisternae of rough endoplasmic reticulum (rER) (8). In fact, most of the space in the supranuclear region of the cell is occupied by Golgi apparatus and rER, as confirmed by volume measurements by means of the point-hit method (Table I).

Above the level of the apical terminal web is a broad cytoplasmic extension, the apical or Tomes' process (Fig. 5). Its distal portion is embedded in enamel matrix. Within its central core, toluidine blue–positive material can be seen which is identified in the electron microscope as representing a group of secretory granules (Figs. 6, 12).

The Golgi Apparatus

In three dimensions, the Golgi apparatus resembles a hollow cylinder which encloses a central cytoplasmic core and shows *inner* and *outer* surfaces. When cut in longitudinal section, the ap-

---

[2] Between the region of enamel matrix secretion and the incisal tip of the tooth, the ameloblasts become smaller and acquire different morphological features. They are thought to be involved in processes other than matrix secretion (5, 37–41); nevertheless, recent evidence indicates that they also have a secretory function (42). According to general usage, the term "secretory ameloblast" will be restricted in this report to those cells that elaborate the enamel matrix.

paratus appears as a double array of stacks of saccules, one on either side of the cell axis (Fig. 7). Each array consists of successive stacks of saccules aligned end-to-end in a linear fashion. The stacks are associated with condensing vacuoles, secretory granules, and two different types of coated vesicles: small ones measuring 400–700 A which are covered with rather fine, fuzzy material and will be referred to as "fuzz-coated" (Fig. 8, *I* at center left), and large ones measuring 800–1000 A which are covered with rather thick bristles and will be referred to as "bristle-coated" (Fig. 8, *V*).

Adjacent to the *outer* Golgi surface, the profiles of rER cisternae run parallel to the long axis of the cell. Some of these cisternae possess ribosome-free regions which display fuzz-coated buds (arrows at upper right in Fig. 8). These buds often face Golgi stacks directly. Groups of small vesicles, some of which are partly or completely fuzz-coated, may be seen around Golgi stacks, with predominance in the cleft of cytoplasm that intervenes between the outer Golgi saccules and rER cisternae (Figs. 7, 10, *I*); these are referred to as "intermediate" vesicles. Finally, fuzz-coated buds are also found attached to the outer Golgi saccules (Fig. 8, arrows at upper and lower left; Fig. 10, arrows); these are also similar in appearance and dimension to intermediate vesicles.

The number of Golgi saccules per stack varies from two to six, with four being the usual number. Outer saccules display well-defined fenestrations when sectioned face-on (Fig. 8, S_2 at lower left). Fenestrations may also be recognized in cross-section (Fig. 10). The outer saccules have a wide lumen and usually lack discernible internal content, whereas those located in the middle of a stack tend to be more flattened and have fewer fenestra-

FIGURE 13 Golgi region. On either side, the discontinuous vertical stained line represents cell coat material present in the intercellular space between adjacent ameloblasts. The Golgi apparatus appears as a double array of stained saccules which demarcate a core of cytoplasm containing stained condensing vacuoles (CV) and secretory granules (G). A staining intensity gradient exists among Golgi saccules in a given stack. The outermost saccule (S_1) contains little or no stained material, whereas the other saccules show increasing amounts (S_2–S_4). The stained material within S_4 is similar in its density and texture to that seen within condensing vacuoles. Secretory granules stain more intensely than the vacuoles.

FIGURE 14 Portions of two apical processes and their surrounding enamel matrix. The processes are unstained, except for the secretory granules (G) and structures which may correspond to smooth tubular elements (arrows). The enamel matrix is intensely stained. This staining may be assigned to linear components running parallel to one another.
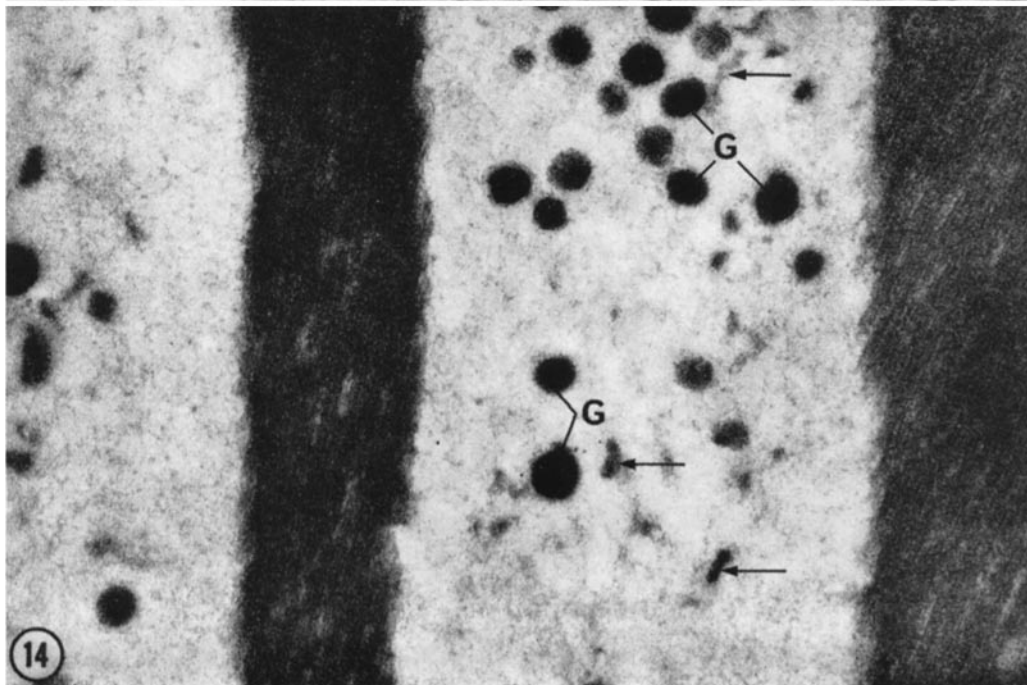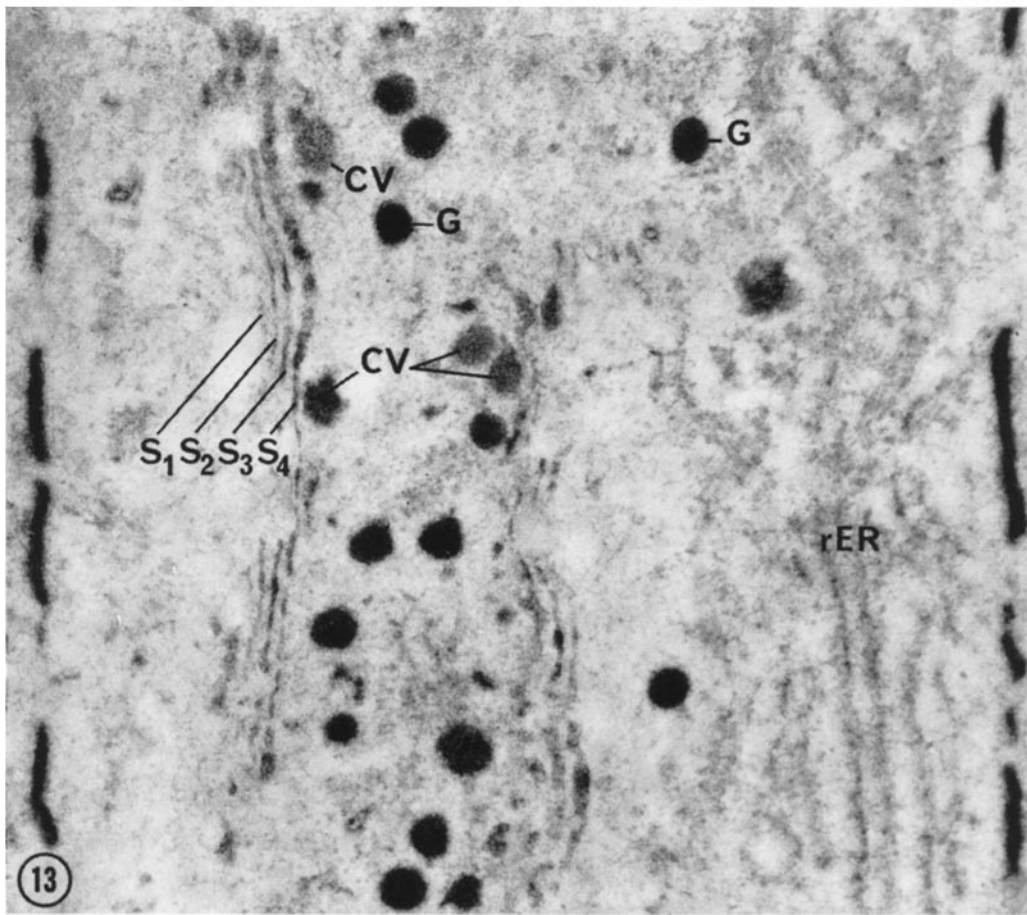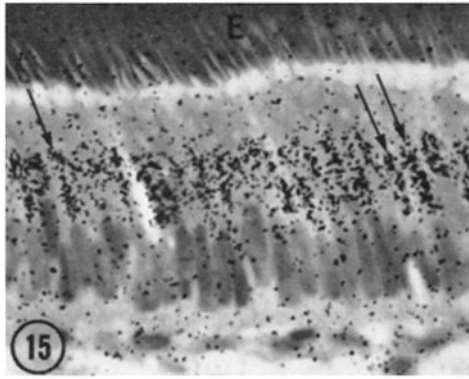
FIGURE 15 Light microscope radioautograph of a paraffin section of secretory ameloblasts 5 min after injection of galactose-³H (200 day exposure). The silver grains are localized in parallel rows (arrows) over the supranuclear region, in correspondence with the location of the Golgi apparatus. (The enamel matrix, E, shows a slight reaction attributed to unspecific adsorption of label.) × 700.
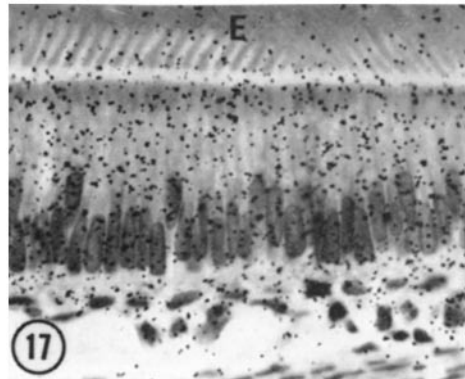
FIGURE 17 Light microscope radioautograph of ameloblasts 2.5 min after glucose-³H injection (104 day exposure). Silver grains appear to be scattered diffusely over the cells, with predominance over basophilic regions. The radioautograph does not show rows of grains over the Golgi region, as observed at early time intervals after galactose-³H (Fig. 15). E, enamel matrix. × 650.
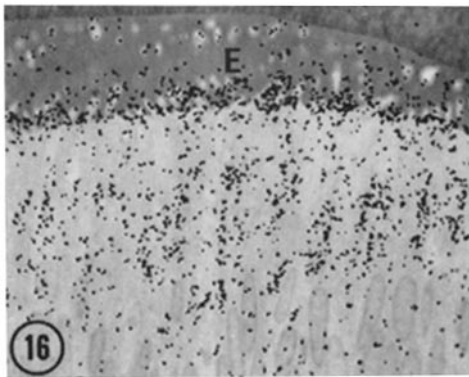

FIGURE 16 Light microscope radioautograph of a semithin Epon section of secretory ameloblasts 20 min after injection of galactose-³H (105 day exposure). Some silver grains are in rows over the Golgi regions and others are scattered over the cell, but the main accumulation of grains is over apical processes and nearby enamel matrix (E). (The light areas seen in the matrix near the top of the picture are tips of apical processes; each shows a few overlying grains.) × 650.

tions and a denser content than the outer ones (Fig. 10, S_3 and S_4). The innermost saccule may, in some instances, appear flattened with few fenestrations, as shown in Fig. 10 (S_5), or may appear irregularly distended and filled with an electron-opaque material (Fig. 11, upper right). Indeed, it is not uncommon to observe the internal content of the innermost saccules arranged in localized swellings resembling a string of beads. Five such swellings, connected by attenuated remnants of the saccule, can be seen in the center of Fig. 9. Each of these swellings exhibits an irregular halo which separates the loosely applied saccular membrane from the condensed material within. By analogy with what is observed in the pancreatic acinar cell, they are referred to as "condensing vacuoles." Besides these saccule-bound condensing vacuoles, many others appear free in the cytoplasm.

The free condensing vacuoles (1500–2000 A in diameter) are composed of granular or homogeneous material surrounded by an uneven electron-

FIGURE 18 Radioautograph obtained 2.5 min after injection of galactose-³H (5 month exposure). The silver grains are over the Golgi apparatus with some predominance over outermost saccules in the cell at left. The lower grains in the central cell are associated with innermost saccules. The rER, condensing vacuoles (CV), and secretory granules (G) are unlabeled. × 28,000.

FIGURE 19 Radioautograph obtained 2.5 min after injection of galactose-³H (5 month exposure). At lower left, a grain is situated over Golgi saccules. At upper right, a group of grains overlaps an innermost saccule and vesicles, while the single grain is over an intermediate vesicle. The grain at lower right seems to be over ribosomes. G, secretory granule. × 35,000.
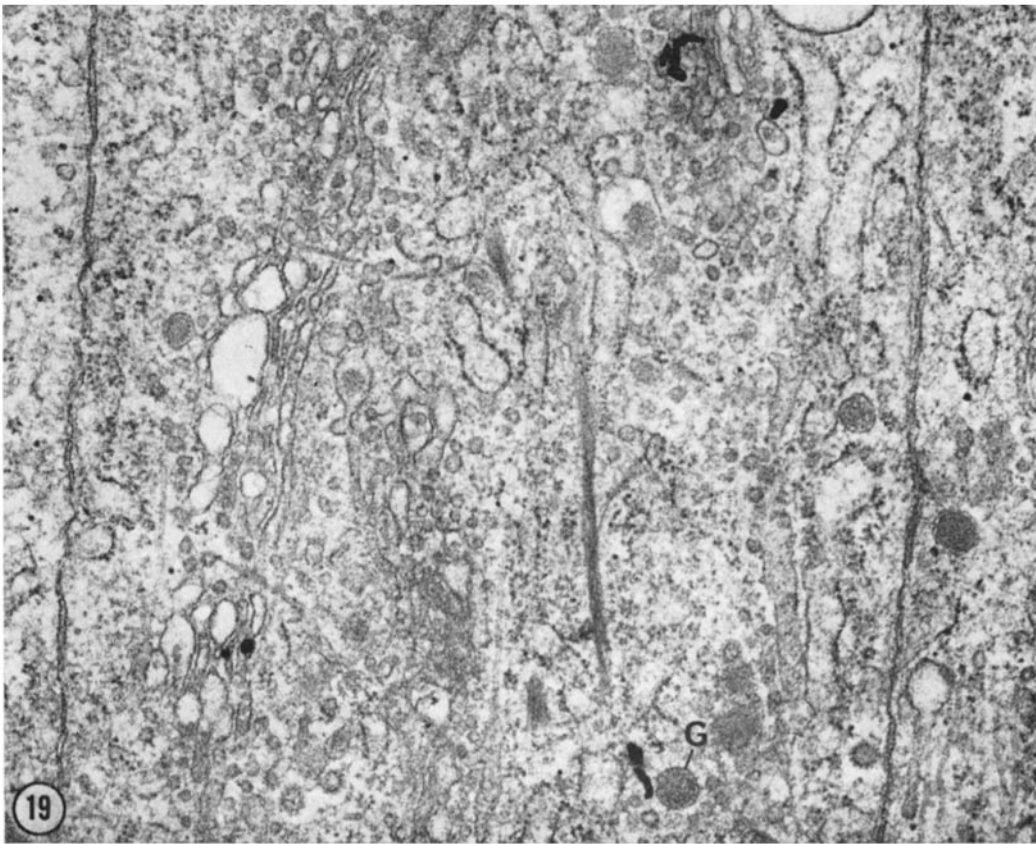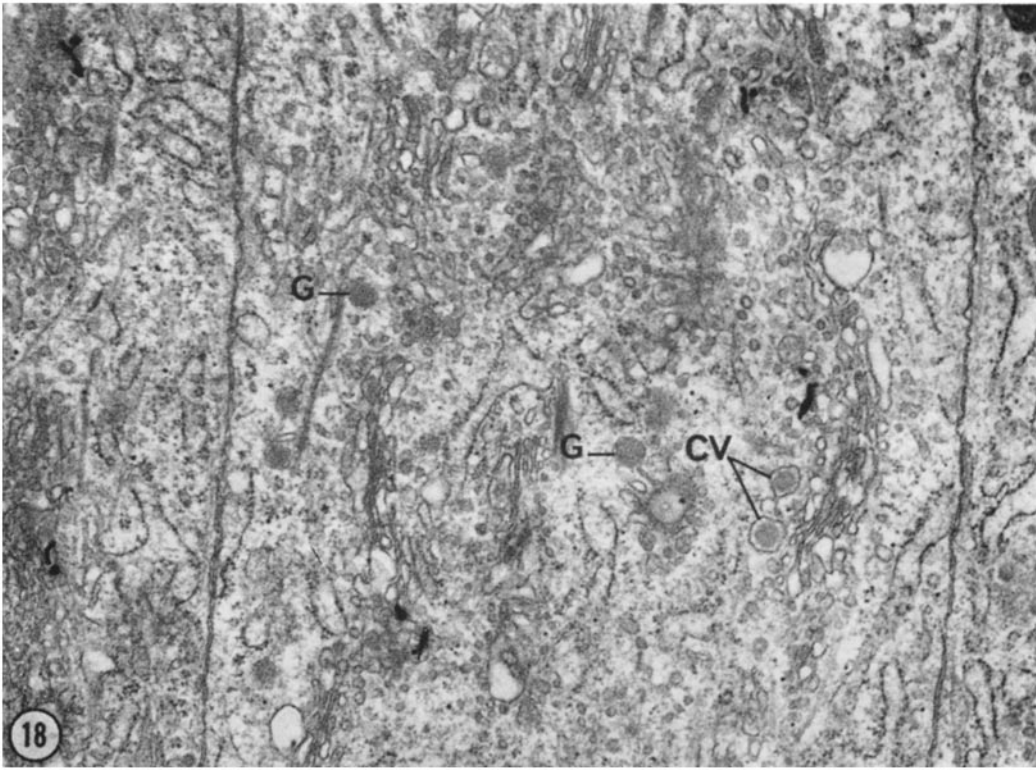
lucent halo and a loosely fitting membrane (Fig. 8). They are usually found on the inner aspect of Golgi stacks or at least within the axial core of cytoplasm enclosed by the two arrays of Golgi saccules. In this region an occasional cisterna of rER as well as intermediate vesicles may also be present. Bristle-coated vesicles are fairly common (V in Figs. 7-9 and 11). Occasionally the membrane of condensing vacuoles displays limited areas with a similar bristle coating (Fig. 8, arrowhead at upper center) or possesses distinct coated buds (Fig. 11, arrows).

Finally, the Golgi region contains structures which resemble condensing vacuoles but are somewhat smaller and rounder (1200-1700 A in diameter), have their membrane more tightly applied, and usually display a more homogeneous content. Again by analogy with the pancreatic acinar cell, these are considered to be *secretory granules*. They may be seen in the central core (Fig. 7, lower center) as well as outside the Golgi region (Fig. 7), but are particularly numerous in the apical process (Fig. 12).

The Apical (Tomes') Process and the Nearby Enamel Matrix

The Golgi apparatus is separated from the apical process by a short region packed with rER cisternae (Fig. 6). The apical process itself is composed of two parts: a *proximal* one in contact on all sides with other ameloblasts, and a *distal* one embedded within prongs of enamel matrix.

The proximal part of the apical processes (Fig. 12) contains a few secretory granules among several cytoplasmic components, namely smooth tubular and vesicular structures with occasional ribosomes, microtubules, glycogen granules, and multivesicular bodies (Fig. 6). Bristle-coated vesicles are often found next to the lateral plasma membrane (Fig. 12, V).

The distal part contains similar structures but with two main differences. First, secretory granules occur in large numbers (condensing vacuoles are rare), and second, these granules together with microtubules and other elements are restricted to the central core of the process. This core is ensheathed by a feltwork of packed filaments (Fig. 12, f) except at the distal end where its contents come close to the plasma membrane. There, the plasma membrane is often thrown into elaborate folds which invaginate into the cytoplasm (horizontal arrows at top of Fig. 12) and often display a bristle coating at their leading edge. Both membrane and folds are closely associated with secretory granules as well as coated vesicles.

Similarly, at the proximal tips of the prongs of matrix, there are conspicuous membrane infoldings which are associated with secretory granules and coated vesicles (Figs. 6 and 12).

The two parts of the apical process referred to above face regions of the enamel matrix with a unique morphology (double and single asterisks in Fig. 12). These two regions have a slightly lower density than the rest of the matrix and often appear striated. When the plane of section is optimal, they show loosely packed, parallel, linear subunits ending next to the plasma membrane (Fig. 23, right). For reasons that will be made clear below, these two parts of the matrix are referred to as "growth regions" (Fig. 6).

DETECTION OF GLYCOPROTEIN BY PHOSPHOTUNGSTIC ACID AT LOW pH

When thin sections of glycol methacrylate-embedded ameloblasts were treated with phosphotungstic acid at low pH (21) for the detection of glycoprotein (22), the content of Golgi saccules was stained. However, the outermost saccule in a stack exhibited little or no reactive content (Fig. 13, S_1). A gradient of increasing staining intensity, perhaps due to filling of the saccules, was observed in the stacks up to the innermost saccule, which displayed a relatively large amount of stained material (Fig. 13, S_4). This material was of a density and texture similar to that observed in nearby spherical structures which, because of their location and size, were identified as condensing vacuoles. Scattered within and outside the Golgi region were more intensely stained, smaller

---

FIGURE 20 Radioautograph obtained 5 *min* after injection of galactose-^{3}H (9 month exposure). All silver grains overlap Golgi saccules, some of which are tangentially cut. The grain at lower right is partly over a condensing vacuole. × 35,000.
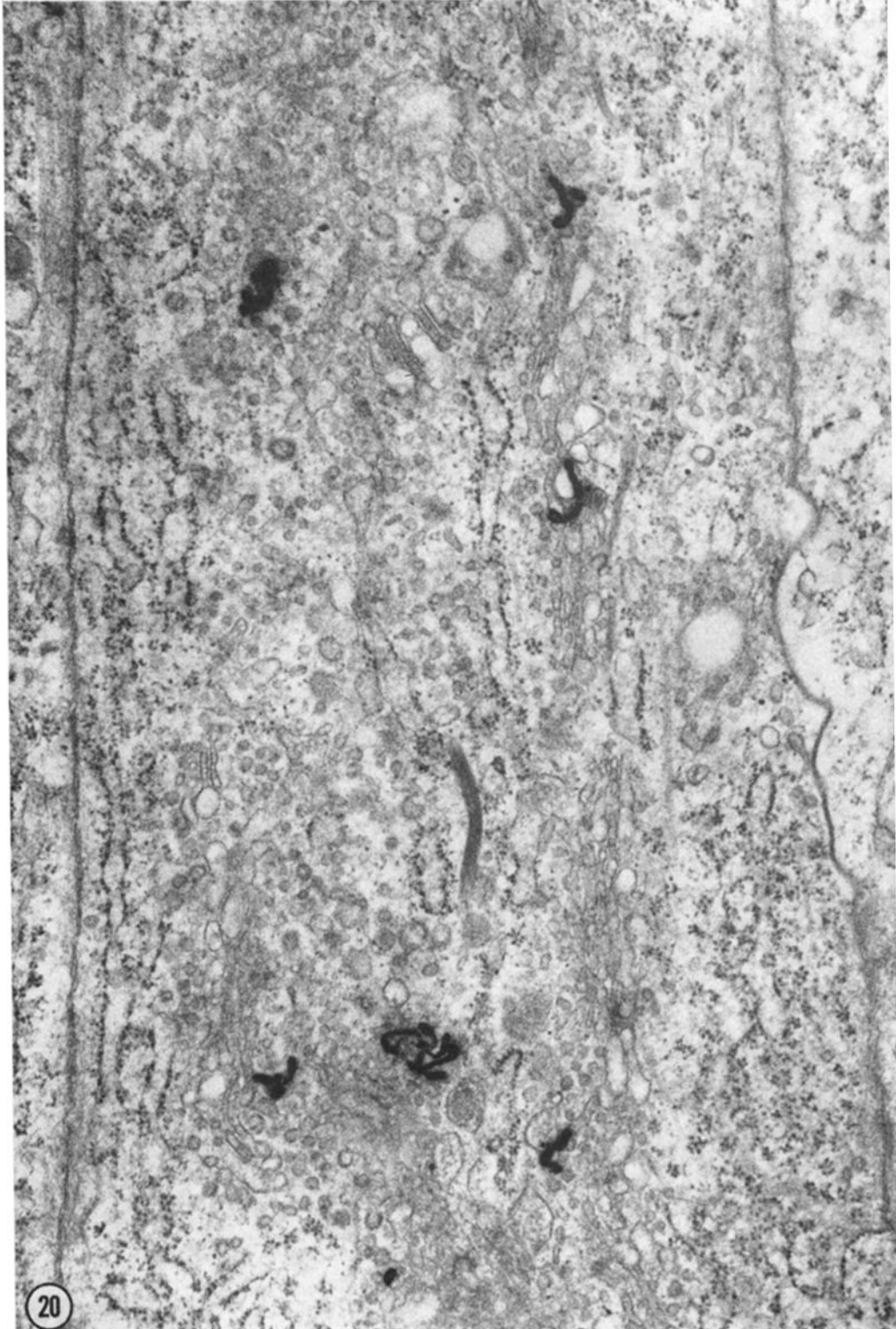
spherical structures which were taken to be secretory granules. Indeed, these stained like the readily identified secretory granules of the apical process (Fig. 14). Finally, the enamel matrix itself took up the stain. The staining was examined in the region of the apical processes and was assigned to linear subunits. The subunits appeared to be loosely packed in the growth regions where they were readily seen with routine stains, and closely packed in the rest of the matrix where they could be detected with routine stains only at relatively high magnification.

RADIOAUTOGRAPHY

Light Microscopy

At *2.5 and 5 min after injection of galactose-³H*, light microscope radioautographs demonstrated a reaction over the supranuclear cytoplasm of ameloblasts[3]. Most silver grains were localized in elongated rows or clusters over the region of the cell corresponding to the location of the Golgi apparatus. While the reaction was stronger at 5 than at 2.5 min after injection, the patterns were similar (Fig. 15). Little change was seen at *10 min*, but at *20 and 30 min* the majority of the grains was over the apical processes and associated matrix (Fig. 16).

When, for comparison, *glucose-³H* was injected, a fairly diffuse reaction was observed 2.5 and 5 min later, with predominance of the silver grains over

---

[3] At 2.5 and 5 min after injection, scattered silver grains were observed over the whole enamel matrix, whether glutaraldehyde or paraformaldehyde was used for fixation. This reaction diminished rapidly with time and was attributed to nonspecific binding of labeled galactose. Addition of nonradioactive galactose to the fixative reduced this effect.

the basophilic areas along the sides of, and above the Golgi region (Fig. 17).

Electron Microscopy

Radioautographs of ameloblasts obtained at *2.5 min* after galactose-³H injection demonstrated silver grains over the Golgi apparatus (Figs. 18 and 19). Most of the grains were restricted to the stacks of saccules. It was thought that grains were distributed with the same frequency over any one of the four saccules constituting an average stack. A few grains were also observed over groups of intermediate vesicles (Fig. 18). Occasional grains were seen over condensing vacuoles. The expanse of cytoplasm occupied by the rER was either devoid of label or infrequently showed a scattered grain.

At *5 min* postinjection, the silver grains were more numerous than at 2.5 min, but were again mostly localized over Golgi saccules (Fig. 20). A few grains were seen over condensing vacuoles.

At the *10 min* interval, a strong radioautographic reaction persisted over the Golgi stacks, but, in addition, fairly numerous grains were detected over the condensing vacuoles and secretory granules of the Golgi region (Fig. 21). Secretory granules in the apical processes were essentially label-free at this time. When radioautographs of ameloblasts incubated with α-amylase were examined in the electron microscope, it was found that this treatment had no effect on the radioautographic reaction (Fig. 22), indicating that the Golgi-localized reaction was not attributable to nearby glycogen granules.

By *20–30 min* after galactose-³H injection, there was a persistence of a Golgi reaction and some increase in the labeling of the rER, but more striking was the appearance of silver grains over the apical

---

FIGURE 21 Radioautograph obtained *10 min* following galactose-³H injection (6 month exposure). In the lower right quadrant, two condensing vacuoles (*CV*) are each overlaid by a silver grain. At upper right, two secretory granules (*G*) are also under silver grains. The other grains nearby are over Golgi saccules. The cell at left (separated by the adjacent cell membranes, *CM*) shows grains over obliquely cut Golgi saccules. Finally, two small grains at right are over ribosomes. × 21,500.

FIGURE 22 Radioautograph obtained *10 min* after injection of galactose-³H (Gevaert 307 emulsion, 6 month exposure). This specimen had been fixed in paraformaldehyde and incubated in an α-amylase solution for 1 hr at 37°C before embedding in Epon, in order to extract glycogen. Four silver grains are visible. The three grains at left are located over Golgi saccules (from top to bottom respectively over the second, fourth, and first saccule). The grain at upper right is over an unidentified component of the Golgi region. × 40,000.
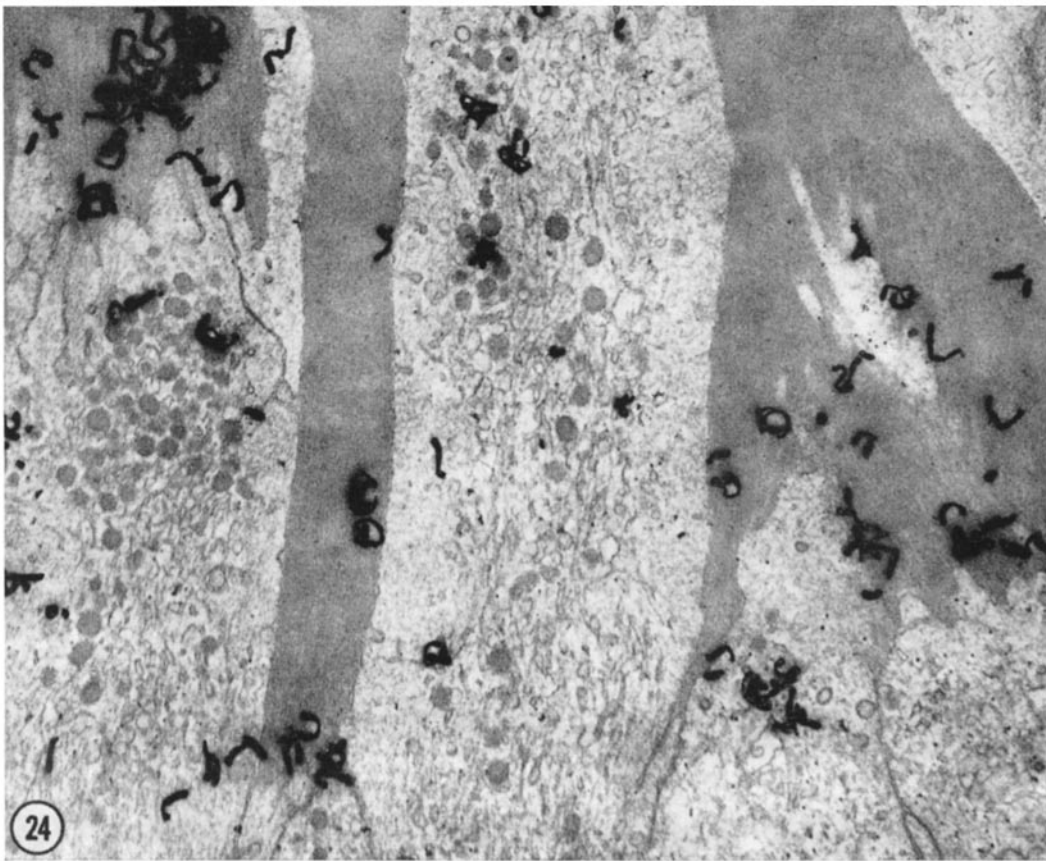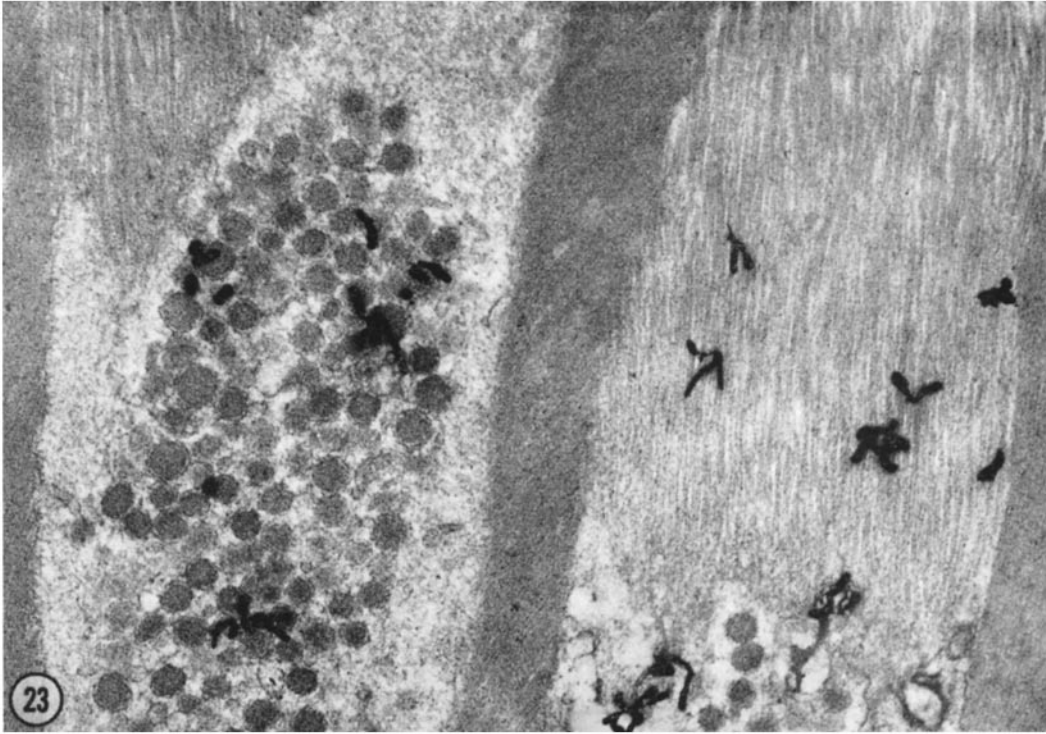
43
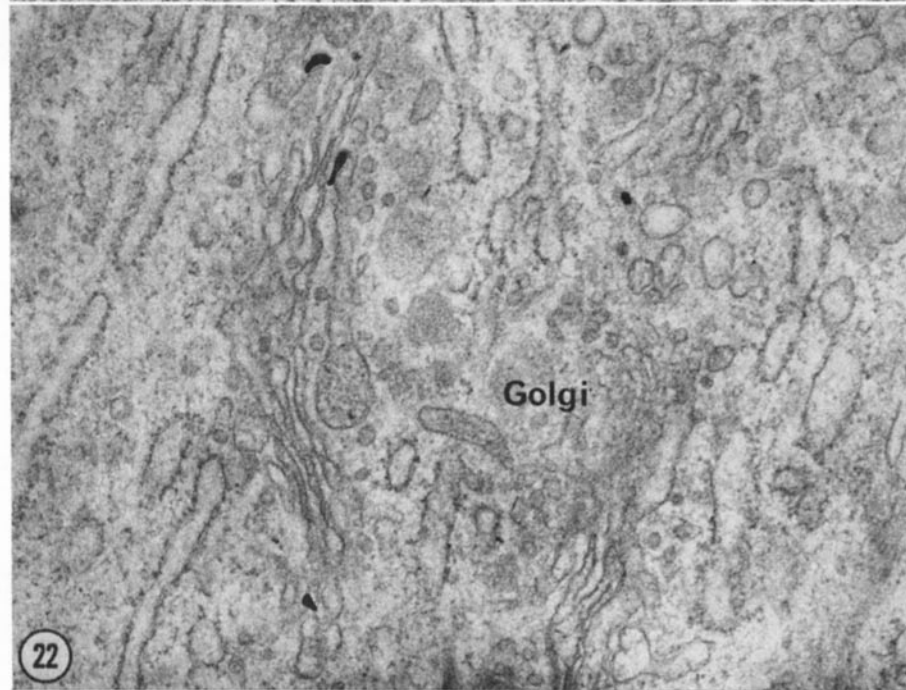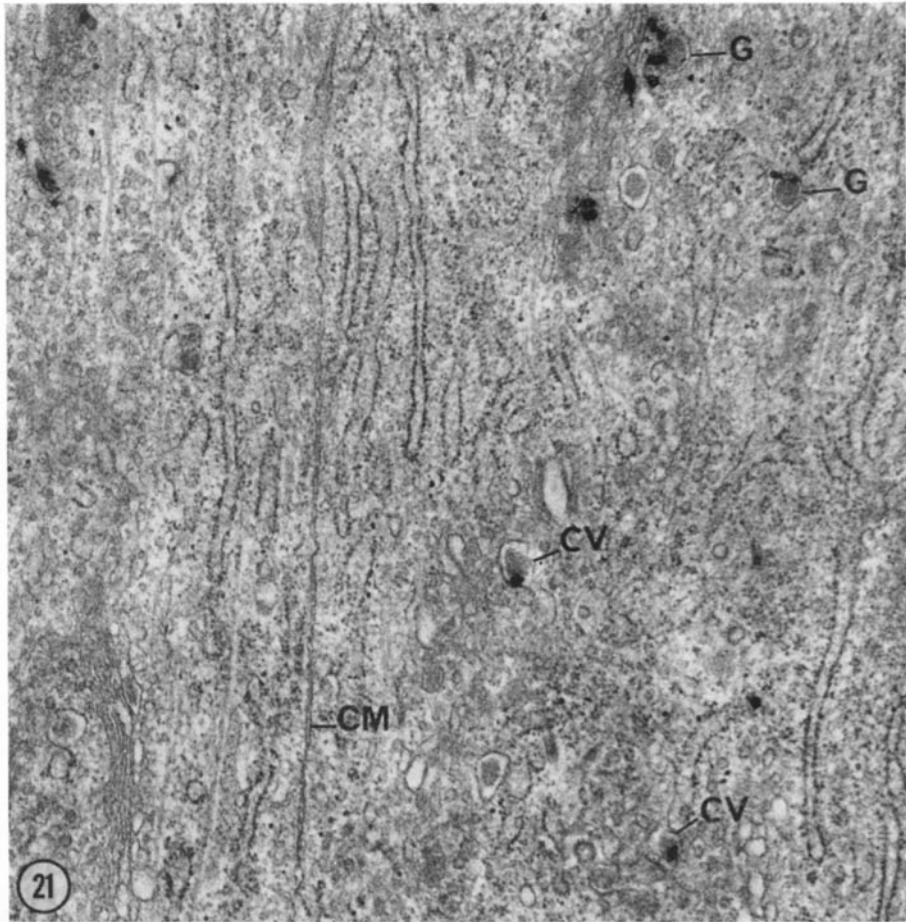
TABLE II

Quantitation of Silver Grains

Time after galactose-³H injection	Grains	Grains over				
		rER	Golgi apparatus	Secretory granules + condensing vacuoles	Matrix	Other structures
min	*No.*	%	%	%	%	%
2.5	145	9	75	12	—	4
5	273	13	66	17	—	4
10	261	19	45	29	—	7
30	1029	18	20	23	21	18

processes and parts of the enamel matrix. In the apical processes, silver grains predominated over the secretory granules accumulated therein (Fig. 23). The enamel matrix exhibited silver grains mainly over the growth regions, that is, above the ends of the apical processes (Fig. 23), and at the tips of the enamel prongs projecting between these processes.

Quantitative Radioautography

The quantitative results (Table II) confirmed that at 2.5 min after galactose-³H injection, most of the radioactivity was in the Golgi apparatus, although a small fraction was in condensing vacuoles and rER. At *5 min* postinjection, the largest grain distribution was still over the Golgi apparatus, but more grains were associated with condensing vacuoles and secretory granules. This phenomenon was accentuated at the *10 min* interval. By *30 min* after the injection, the distribution of grains over the Golgi apparatus was relatively less than at earlier intervals. However, by this time much of the

radioactivity had migrated *outside* of the supranuclear region, since it appeared in the secretory granules of the apical processes as well as in the enamel matrix.

DISCUSSION

Presence of Glycoprotein in the Organic Matrix of Enamel

The organic matrix constitutes approximately 20% of the enamel in embryonic teeth (43–46), but only 0.5% in the adult when mineralization is completed (12, 47–49). The matrix is mainly composed of protein (45, 50–53) with 1.5–2% carbohydrates in mature human and bovine enamel (12, 13, 54) and 1% in embryonic bovine enamel (17). The carbohydrates are in the form of glycoprotein (12–17) and mucopolysaccharide (15).

Two glycoprotein-containing fractions have been isolated from mature bovine enamel matrix. One contains galactose, glucose, mannose, and fucose, and the other contains galactose as the only

---

FIGURE 23 Radioautograph of portions of the apical (Tomes') processes of two secretory ameloblasts and adjacent enamel matrix obtained at *30 min* after injection of galactose-³H (3 month exposure). Uranyl acetate and lead citrate. This figure shows from left to right: (*a*) an enamel prong separating apical processes; (*b*) an apical process containing a large number of secretory granules and facing a small portion of striated matrix (upper left); (*c*) another enamel prong; (*d*) the distal end of an apical process with secretory granules at lower right, and above it, a large portion of striated matrix. The silver grains are found in two locations: over the groups of secretory granules; and over the regions of striated matrix, as shown at right. × 33,000.

FIGURE 24 Radioautograph of apical processes of secretory ameloblasts and adjacent matrix *4 hr* after injection of fucose-³H (2 month exposure). At this time, some silver grains are left over secretory granules. Most of the grains are over the two striated regions of enamel, that is, next to the distal ends of apical processes (upper left) and at the tips of the enamel prongs (lower left and right of figure). These are, therefore, referred to as "growth regions." × 20,000.

hexose, while glucosamine and galactosamine are present in both (16). A hexosamine-containing glycoprotein has also been found in human enamel (15).

The embryonic bovine enamel matrix, which is similar to the rat enamel matrix in amino acid composition (55), contains a fraction soluble in acid and one soluble at neutral pH (52). Both include galactose and galactosamine. The acid-soluble fraction, believed to be derived from rod sheaths (56), contains galactose as the only hexose. The fraction soluble at neutral pH, believed to consist of the rods themselves, includes 75% of its hexoses as galactose, with the rest as glucose and mannose (17).

When sections of enamel matrix were stained by the low-pH phosphotungstic acid technique which is reasonably specific for the detection of glycoprotein (22), parallel linear structures reacted (Fig. 14). Judging from their size, these represented the long tubular subunits previously described in the enamel matrix (57, 58). These subunits should, therefore, contain glycoprotein material, presumably including galactose, since this sugar was found in all the glycoprotein fractions of enamel in which its presence was investigated.

Availability of Galactose after Intravenous Injection

With time after intravenous injection of galactose-³H, the radioactivity in blood plasma fell rapidly (Fig. 1). Furthermore, only about one-half of the labeled hexose was in the form of galactose at 2 min, and less than one-sixth at 10 min after injection (Figs. 2 and 3). Hence, the injected galactose-³H left the blood rapidly and, presumably, the pulse available to the tissues was brief. Furthermore, since only traces of galactose are normally present in rat blood (59), the specific activity of the blood galactose during the pulse must have been high, nearly as high as that of the injected material.

The drop in the radioactive galactose of blood plasma was associated with the appearance of radioactive glucose (Figs. 2 and 3). A transformation of galactose into glucose may take place in the cells of liver, and perhaps other organs, by conversion of galactose to uridine diphosphate galactose (UDP-galactose) (60), which in turn transforms into UDP-glucose (61), which finally yields free glucose (62). Nevertheless, because of its dilution by preexisting liver and blood glucose,

the labeled glucose derived from galactose should have a relatively low specific activity and, therefore, exert much less influence on the radioautographic reaction pattern than the label present at early times as high specific activity galactose.

Site of Galactose Incorporation into Glycoprotein

It may first be recalled that the site of protein synthesis in ameloblasts, as in other cells, is the rER, as was demonstrated by radioautography within minutes after tyrosine-³H injection (63). At later time intervals, the newly synthesized protein migrated to the Golgi apparatus and later still to the matrix (63). In this regard, the membranous buds seen on rER cisternae (Fig. 8, upper right) were often attached by long stems and possessed a fuzzy coating. The stems suggested extrusion of membrane rather than fusion and, therefore, the buds are believed to give rise to the nearby intermediate vesicles. Furthermore, buds with a fuzzy coating but often lacking stems were present on outer Golgi saccules (Fig. 10), suggesting fusion of vesicles with these saccules. Briefly, it is thought that the intermediate vesicles transfer newly synthesized protein from the rER to the Golgi apparatus, as is indeed believed to occur in other cells.

The problem at hand was to investigate the intracellular location at which galactose and some of the other sugar residues identified in enamel glycoprotein, namely, glucose, mannose, hexosamine, and fucose (16), became incorporated into forming glycoproteins. The information available on the uptake of most of these sugar residues by the ameloblasts was limited except for galactose. Glucose label was shown to be taken up into the basophilic regions of these cells (Fig. 17), that is, within the rER. Hence, glucose may be incorporated there into glycoprotein; yet, this readily metabolized sugar may also give rise to small carbon fragments which would contribute to the formation of amino acids, which in turn would be synthesized into protein in the rER. However, it was known that the label of bicarbonate-¹⁴C, a small carbon fragment, was not incorporated into enamel by ameloblasts, whereas the label of glucose-¹⁴C was taken up by these cells (66). Similar observations with mannose-¹⁴C (66) also suggested that this sugar was taken up into ameloblasts. Recently, preliminary results obtained after

mannose-^{3}H injection indicated that this sugar may be incorporated into the rER (67). Briefly, the material migrating to the Golgi apparatus would consist of incomplete glycoprotein molecules carrying carbohydrate side chains which include glucose and mannose residues.

The radioautographs obtained 2.5 min after galactose-^{3}H injection showed the presence of radioactivity within the Golgi apparatus (Figs. 18, 19; Table II). This finding implied that the labeled galactose, after being transformed into UDP-galactose, was incorporated into glycoprotein or, possibly, glycogen (68–71). Uptake into glycogen was ruled out since extraction of this substance by α-amylase did not seem to influence the radioautographic pattern (Fig. 22). The Golgi labeling would, therefore, be due to galactose incorporation into glycoprotein.[4] Galactose would have to be inserted into the proper sequence within the growing carbohydrate side chains of the incomplete glycoprotein, a step requiring the presence of the enzyme galactosyltransferase. This enzyme has been detected in Golgi fractions of liver (76, 77), where the Golgi uptake of galactose label has also been demonstrated (73).

Finally, there was evidence that fucose and perhaps glucosamine were also incorporated into the Golgi apparatus of ameloblasts (67). The fact that fucose is located at the terminal end of the carbohydrate side chains in many glycoproteins would indicate that, after the successive addition of glucose, mannose, glucosamine, and galactose, some side chains are completed in the Golgi apparatus by the incorporation of fucose. In this regard, the sequence of the sugar residues in the carbohydrate side chains of enamel matrix glycoprotein is unknown; however, it is noteworthy that in the follicular cells of the thyroid gland, the rER is the site of uptake of mannose (64), whose location in the carbohydrate side chains of thyroglobulin is close to the protein moiety, whereas the Golgi apparatus is the site of uptake of galactose (64), which is located near the end of the side chains, and fucose (65) which occupies a terminal position.

In the hope of pinpointing the sites of uptake of galactose-^{3}H, special attention was given to the radioautographs prepared 2.5 min after galactose-^{3}H injection. The silver grains occurred with equal

---

[4] The uptake of galactose label into the Golgi apparatus was also observed in goblet cells (72), liver cells (73), columnar cells of the intestine (74), and lymphocytes (75).

frequency over all the saccules, usually four, which make up a Golgi stack, so that all would participate in incorporating galactose into glycoprotein. On the other hand, the histochemical staining for glycoprotein showed an increasing gradient from outer to inner saccules (Fig. 13). These two observations may be reconciled by assuming that Golgi saccules are dynamic structures arising on the outside of the stack and migrating inwards while accumulating glycoprotein. This view implied a continuous renewal of Golgi saccules, as proposed earler for the intestinal goblet cell (78).

At the 2.5 min time interval, a few silver grains were also over rER (Table II) and intermediate vesicles (Fig. 18). These reactions might be caused by the labeled glucose derived from labeled galactose (Fig. 3), since, after direct injection of glucose-^{3}H, the reactions predominated over the basophilic regions of the cell (Fig. 17), that is, over the rER. Another possible explanation of rER reaction is suggested by the fact that much of the rER reaction was over cisternae abutting directly on the Golgi zone. Perhaps galactosyltransferase is also located within intermediate vesicles and adjacent rER, resulting in some addition of labeled galactose to forming glycoprotein at these sites.

Although occasional silver grains were seen at 2.5 min over condensing vacuoles (Table II), it was not clear whether these structures themselves took up galactose. In each case they were located next to innermost Golgi saccules which might have been the source of radioactivity. We are inclined to believe that, if any uptake of label occurs in condensing vacuoles, this uptake is only slight.

Migration of the Galactose-^{3}H Labeled Glycoprotein

On the other hand, by 5 min and especially by 10 min after injection, the frequency of silver grains over condensing vacuoles was increased (Fig. 21). Some of the grains were over condensing vacuoles which were not near innermost saccules. The interpretation was that the glycoprotein synthesized in Golgi saccules had found its way into condensing vacuoles. Morphological features confirmed this conclusion, to wit: the content of condensing vacuoles was similar in density and texture to that of many innermost saccules (Fig. 11); both contained glycoprotein (Fig. 13); and Fig. 9 provided good evidence that innermost saccules evolved into condensing vacuoles. It may be speculated that, when

an innermost saccule disappears in this manner, this saccule is soon replaced by the evolution of the next saccule. In fact, throughout the stack, each saccule would take the place of the next inner one, while on the outer side a new outermost saccule would be formed, thus insuring continuous renewal of Golgi stacks.

At a next step, condensing vacuoles would transform into secretory granules since, by the 10 min interval, secretory granules were frequently labeled (Fig. 21). Even though condensing vacuoles and secretory granules together occupied only 2.3% of the volume of the supranuclear region (Table I), they contained 29% of its radioactivity at 10 min (Table II). Incidentally, when the vacuoles "condensed" into the secretory granules, their size decreased (as shown at the base of Fig. 8) and their surface was reduced by about one third, so that the excess membrane would have to be disposed of in some manner. We believe that this is done by the formation of coated buds with long stems (Fig. 11) and their subsequent extrusion as coated vesicles. The fate of these coated vesicles was unknown; perhaps they were taken into the multivesicular or dense bodies that are commonly seen in this region of the cell (Fig. 9).

Condensing vacuoles were more numerous than secretory granules in the Golgi region, but only the latter were found in abundance in the apical processes. There they became labeled as early as 20–30 min after galactose-³H injection (Figs. 16, 23). It was, therefore, likely that secretory granules left the Golgi region soon after they evolved from condensing vacuoles and that they rapidly traveled the distance to the apical process.

Sites of Secretion of Glycoprotein Outside the Cell

At 20 min and especially at 30 min after injection of galactose-³H, the label appeared over the enamel matrix (Fig. 23; Table II), indicating that the glycoprotein content of secretory granules had been released by the cells to the matrix. The deposition took place mostly in two regions of the matrix: that abutting against the distal end of apical processes and that at the tips of the prongs separating these processes. The deposition of label in these two regions may be illustrated at 4 hr by a micrograph from unpublished work with a glycoprotein precursor which is more stable than galactose over this period of time and behaves in a similar man-

ner, fucose-³H (Fig. 24). Because of deposition of glycoprotein in these two parts of the matrix, they may be referred to as the "growth regions" of developing enamel.

The precise mode of discharge of the granule contents is not clear. Some images suggested, although not decisively, that secretory granules may release their content by exocytosis at the surfaces facing the two growth regions and perhaps into the associated membranous folds. An excess of membrane would result from such exocytosis. We believe that the presence of bristle-coated buds with long stems attached to the surface membrane and its folds suggests that excess membrane is released back into the cell in the form of bristle-coated vesicles. These vesicles might be collected into the multivesicular bodies commonly found in the apical process.

Whatever the mode of discharge, the appearance of radioactivity within the enamel of the growth regions demonstrated that the glycoprotein is released from secretory granules and deposited as enamel matrix. Since the linear subunits of the matrix contain glycoprotein, it is likely that the new glycoprotein molecules are added on to the free ends of the subunits adjacent to the plasma membrane, thus accounting for their continuous elongation during matrix formation.

REFERENCES

1. FEARNHEAD, R. W. 1960. Mineralization of rat enamel. *Nature (London).* 188:509.
2. FEARNHEAD, R. W. 1961 *a.* Electron microscopy

of forming enamel. *Arch. Oral Biol.* (Suppl.) **4**:24.

3. FEARNHEAD, R. W. 1961 *b*. Secretory products of ameloblasts. *In* Electron Microscopy in Anatomy. J. D. Boyd, F. R. Johnson, and J. D. Lever, editors. Edward Arnold Publishers Ltd., London. 241.

4. REITH, E. J. 1960. The ultrastructure of ameloblasts from the growing end of rat incisors. *Arch. Oral. Biol.* **2**:253.

5. REITH, E. J. 1961. The ultrastructure of ameloblasts during matrix formation and the maturation of enamel. *J. Biophys. Biochem. Cytol.* **9**:825.

6. WATSON, M. L. 1960. The extracellular nature of enamel in the rat. *J. Biophys. Biochem. Cytol.* **7**:489.

7. KALLENBACH, E., E. SANDBORN, and H. WARSHAWSKY. 1963. The Golgi apparatus of the ameloblast of the rat at the stage of enamel matrix formation. *J. Cell Biol.* **16**:629.

8. WARSHAWSKY, H. 1968. The fine structure of secretory ameloblasts in rat incisors. *Anat. Rec.* **161**:211.

9. JESSEN, H. 1968. The morphology and distribution of mitochondria in ameloblasts with special reference to a helix-containing type. *J. Ultrastruct. Res.* **22**:120.

10. NYLEN, M. U., and D. B. SCOTT. 1960. Electron microscopic studies of odontogenesis. *J. Indiana St. Dent. Ass.* **39**:406.

11. GARANT, P. R., and J. NALBANDIAN. 1968. Observations on the ultrastructure of ameloblasts with special reference to the Golgi complex and related components. *J. Ultrastruct. Res.* **23**:427.

12. STACK, M. V. 1954. Organic constituents of enamel. *J. Amer. Dent. Ass.* **48**:297.

13. EGYEDI, H., and M. V. STACK. 1956. The carbohydrate content of enamel. *N. Y. J. Dent.* **22**:386.

14. BURGESS, R. C., G. NIKIFORUK, and C. MACLAREN. 1960. Chromatographic studies of carbohydrate components of enamel. *Arch. Oral Biol.* **3**:8.

15. CLARK, R. D., J. G. SMITH, and E. A. DAVIDSON. 1965. Hexosamine and acid glycosaminoglycans in human teeth. *Biochim. Biophys. Acta.* **101**:267.

16. GLIMCHER, M. J., and P. T. LEVINE. 1966. Studies of the proteins, peptides and free amino acids of mature bovine enamel. *Biochem. J.* **98**:742.

17. SEYER, J., and M. J. GLIMCHER. 1969. The content and nature of the carbohydrate components of the organic matrix of embryonic bovine enamel. *Biochim. Biophys. Acta.* **184**:509.

18. PEASE, D. C. 1966. Polysaccharides associated with the exterior surface of epithelial cells: kidney, intestine, brain. *J. Ultrastruct. Res.* **15**:555.

19. MARINOZZI, V. 1967. Réaction de l'acide phosphotungstique avec la mucine et les glycoprotéines des plasmamembranes. *J. Microsc. (Paris).* **6**:68a.

20. MARINOZZI, V. 1968. Phosphotungstic acid (PTA) as a stain for polysaccharides and glycoproteins in electron microscopy. 4th *Eur. Reg. Conf. Electron Microsc.* **2**:55.

21. RAMBOURG, A. 1967. Détection des glycoprotéines en microscopie électronique: coloration de la surface cellulaire et de l'appareil de Golgi par un mélange acide chromique-phosphotungstique. *C. R. Acad. Sci. Ser. D.* **265**:1426.

22. RAMBOURG, A. 1969. Localisation ultrastructurale et nature du matériel coloré au niveau de la surface cellulaire par le mélange chromique-phosphotungstique. *J. Microsc. (Paris).* **8**:325.

23. WARSHAWSKY, H., and G. MOORE. 1967. A technique for the fixation and decalcification of rat incisors for electron microscopy. *J. Histochem. Cytochem.* **15**:542.

24. REYNOLDS, E. S. 1963. The use of lead citrate at high pH as an electron-opaque stain in electron microscopy. *J. Cell Biol.* **17**:208.

25. KOPRIWA, B. M. 1966. A semiautomatic instrument for the radioautographic coating technique. *J. Histochem. Cytochem.* **14**:923.

26. HORNSBY, K. M. 1958. Basic Photographic Chemistry. The Fountain Press, London. 58.

27. SALPETER, M. M., and L. BACHMANN. 1964. Autoradiography with the electron microscope. A procedure for improving resolution, sensitivity and contrast. *J. Cell Biol.* **22**:469.

28. KOPRIWA, B. M., and C. P. LEBLOND. 1962. Improvements in the coating technique of radioautography. *J. Histochem. Cytochem.* **10**:269.

29. BASERGA, R., and D. MALAMUD. 1969. Autoradiography. Techniques and Application. Harper and Row, Publishers, New York. 254.

30. CHALKLEY, H. W. 1943. Method for the quantitative morphologic analysis of tissues. *J. Nat. Cancer Inst.* **4**:47.

31. NADLER, N. J. 1971. The interpretation of grain counts in electron microscope radioautography. Appendix to the article by Haddad, A., M. Smith, A. Herscovics, N. J. Nadler, and C. P. Leblond. *J. Cell Biol.* **49**:877.

32. LEDUC, E. H., and W. BERNHARD. 1967. Recent modifications of the glycol methacrylate embedding procedure. *J. Ultrastruct. Res.* **19**:196.

33. COIMBRA, A., and C. P. LEBLOND. 1966. Sites of glycogen synthesis in rat liver as shown by

electron microscope radioautography after administration of glucose-^{3}H. *J. Cell Biol.* **30:** 151.

34. BRAY, G. A. 1960. A simple efficient liquid scintillator for counting aqueous solutions in a liquid scintillation counter. *Anal. Biochem.* **1:** 279.

35. JERMYN, M. A., and F. A. ISHERWOOD. 1949. Improved separation of sugars on the paper partition chromatogram. *Biochem. J.* **44:**402.

36. HOUGH, L., J. K. N. JONES, and W. H. WADMAN. 1950. Quantitative analysis of mixtures of sugars by the method of partition chromatography. V. Improved methods for the separation and detection of their methylated derivatives on the paper chromatogram. *J. Chem. Soc. C.* 1702.

37. WASSERMAN, F. 1944. Analysis of the enamel formation in the continuously growing teeth of normal and vitamin C deficient guinea pigs. *J. Dent. Res.* **23:**463.

38. MARSLAND, E. A. 1952. Histological investigation of amelogenesis in rats. II. Maturation. *Brit. Dent. J.* **92:**109.

39. REITH, E. J. 1970. The stages of amelogenesis as observed in molar teeth of young rats. *J. Ultrastruct. Res.* **30:**111.

40. REITH, E. J., and V. F. COTTY. 1967. The absorptive activity of ameloblasts during the maturation of enamel. *Anat. Rec.* **157:**577.

41. KALLENBACH, E. 1970. Fine structure of rat incisor enamel organ during late pigmentation and regression stages. *J. Ultrastruct. Res.* **30:**38.

42. WEINSTOCK, A. 1970. Uptake of ^{3}H-fucose and ^{3}H-galactose label by "resorptive" ameloblsats and its secretion into a periodic acid (PA)–Schiff-positive surface layer during the phase of enamel maturation. *Anat. Rec.* **166:**395.

43. DEAKINS, M. 1942. Changes in the ash, water, and organic content of pig enamel during calcification. *J. Dent. Res.* **21:**429.

44. WEINMANN, J. P., G. D. WESSINGER, and G. REED. 1942. Correlation of chemical and histological investigations on developing enamel. *J. Dent. Res.* **21:**171.

45. EASTOE, J. E. 1960. Organic matrix of tooth enamel. *Nature (London).* **187:**411.

46. BURGESS, R. C., and C. M. MACLAREN. 1965. Proteins in developing bovine enamel. *In* Tooth Enamel. Its Composition, Properties and Fundamental Structure. M. V. Stack and R. W. Fearnhead, editors. John Wright and Sons, Ltd., The Stonebridge Press, Bristol, England. 74.

47. LOSEE, F. L., and W. C. HESS. 1949. The chemical nature of the proteins from human enamel. *J. Dent. Res.* **28:**512.

48. BATTISTONE, G. C., and G. W. BURNETT. 1956. Studies of the composition of teeth. V. Variations in the amino acid composition of dentin and enamel. *J. Dent. Res.* **35:**263.

49. BURNETT, G. W., and J. A. ZENEWITZ. 1958. Studies of the composition of teeth. VIII. The composition of human teeth. *J. Dent. Res.* **37:**590.

50. EASTOE, J. E. 1963. Amino acid composition of proteins from the oral tissues. II. The matrix proteins of dentine and enamel from developing human deciduous teeth. *Arch. Oral Biol.* **8:**633.

51. PIEZ, K. A. 1961. Amino acid composition of some calcified proteins. *Science (Washington).* **134:**841.

52. GLIMCHER, M. J., G. L. MECHANIC, L. C. BONAR, and E. J. DANIEL. 1961. The amino acid composition of the organic matrix of decalcified foetal bovine dental enamel. *J. Biol. Chem.* **236:**3210.

53. GLIMCHER, M. J., G. L. MECHANIC, and U. A. FRIBERG. 1964. The amino acid composition of the matrix and the neutral and acid soluble components of embryonic bovine enamel. *Biochem. J.* **93:**198.

54. PINCUS, P. 1949. Human enamel protein. *Brit. Dent. J.* **86:**226.

55. LEVINE, P. T., and M. J. GLIMCHER. 1965. The isolation and amino acid composition of the organic matrix and neutral soluble proteins of developing rodent enamel. *Arch. Oral Biol.* **10:**753.

56. GLIMCHER, M. J., D. F. TRAVIS, U. A. FRIBERG, and G. L. MECHANIC. 1964. The electron microscopic localization of the neutral soluble proteins of developing bovine enamel. *J. Ultrastruct. Res.* **10:**362.

57. JESSEN, H. 1968. Elliptical tubules as unit structure of forming enamel matrix in the rat. *Arch. Oral Biol.* **13:**351.

58. WARSHAWSKY, H. 1971. A light and electron microscopic study of the nearly mature enamel of rat incisors. *Anat. Rec.* **169:**559.

59. SEGAL, S., and H. BERNSTEIN. 1963. Observations on cataract formation in the newborn offspring of rats fed a high-galactose diet. *J. Pediat.* **62:**363.

60. KALCKAR, H. M. 1958. Uridine-diphosphogalactose: metabolism, enzymology, and biology. *Advan. Enzymol.* **20:**111.

61. KALCKAR, H. M. 1957. Biochemical mutations in man and microorganisms. *Science (Washington).* **125:**105.

62. WEST, E. S., W. R. TODD, H. S. MASON, and J. T. VAN BRUGGEN. 1966. Textbook of Bio-

chemistry. 4th edition. The Macmillan Company, New York.

63. WARSHAWSKY, H. 1966. Steps in the secretion of enamel matrix protein, as shown by electron microscope radioautography of the ameloblasts of rat incisors following ³H-tyrosine injection. *Anat. Rec.* 154:438.

64. WHUR, P., A. HERSCOVICS, and C. P. LEBLOND, 1969. Radioautographic visualization of the incorporation of galactose-³H and mannose-³H by rat thyroids in vitro in relation to the stages of thyroglobulin synthesis. *J. Cell Biol.* 43:289.

65. HADDAD, A., M. SMITH, A. HERSCOVICS, N. J. NADLER, and C. P. LEBLOND. 1971. Radioautographic study of in vivo and in vitro incorporation of fucose-³H into thyroglobulin by rat thyroid follicular cells. *J. Cell Biol.* 49:856.

66. KUMAMOTO, Y., and C. P. LEBLOND. 1958. Visualization of C¹⁴ in the tooth matrix after administration of labeled hexoses. *J. Dent. Res.* 37:147.

67. WEINSTOCK, A. 1969. Sites of synthesis and pathway of migration of glycoprotein in the ameloblast. Ph.D. Thesis, Department of Anatomy, McGill University.

68. KRAUSS, S., and E. J. SARCIONE. 1964. Synthesis of serum haptoglobin by the isolated perfused rat liver. *Biochim. Biophys. Acta.* 90:301.

69. SARCIONE, E. J. 1964. The initial subcellular site of the incorporation of hexoses into liver protein. *J. Biol. Chem.* 239:1686.

70. McGUIRE, E. J., G. W. JOURDIAN, D. M. CARLSON, and S. ROSEMAN. 1965. Incorporation of D-galactose into glycoprotein. *J. Biol. Chem.* 240:PC4112.

71. KALCKAR, H. M. 1965. Galactose metabolism and cell "sociology." *Science (Washington).* 150:305.

72. NEUTRA, M., and C. P. LEBLOND. 1966 *b.* Radioautographic comparison of the uptake of galactose-³H and glucose-³H in the Golgi region of various cells secreting glycoproteins or mucopolysaccharides. *J. Cell Biol.* 30:137.

73. DROZ, B. 1966. Elaboration de glycoprotéines dans l'appareil de Golgi des cellules hépatiques chez le rat; étude radioautographique en microscope électronique après injection de galactose-³H. *C. R. Acad. Sci. Ser. D.* 262:1766.

74. BENNETT, G. 1970. Migration of glycoprotein from Golgi apparatus to cell coat in the columnar cells of the duodenal epithelium. *J. Cell Biol.* 45:668.

75. ROBINEAUX, R., A. ANTEUNIS, C. BONA, and A. ASTISANO. 1969. Localisation par autoradiographie ultrastructurale du galactose-³H dans le lymphocyte transformé. *C. R. Acad. Sci. Ser. D.* 269:1434.

76. FLEISCHER, B., S. FLEISCHER, and H. OZAWA. 1969. Isolation and characterization of Golgi membranes from bovine liver. *J. Cell Biol.* 43:59.

77. MORRE, D. J., L. M. MERLIN, and T. W. KEENAN. 1969. Localization of glycosyl transferase activities in a Golgi apparatus-rich fraction isolated from rat liver. *Biochem. Biophys. Res. Comm.* 37:813.

78. NEUTRA, M., and C. P. LEBLOND. 1966a. Synthesis of the carbohydrate of mucus in the Golgi complex as shown by electron microscope radioautography of goblet cells from rats injected with glucose-³H. *J. Cell Biol.* 30:119.

79. WEINSTOCK, A. 1967. The incorporation of ³H-galactose into complex carbohydrate by ameloblasts of young rats. *Anat. Rec.* 157:341.